EARLY TRIASSIC AGGRADATIONAL AND DEGRADATIONAL LANDSCAPES OF THE KAROO BASIN AND EVIDENCE FOR CLIMATE OSCILLATION FOLLOWING THE P–Tr EVENT

DANIEL W. PACE,[1]* ROBERT A. GASTALDO,[1] AND JOHANN NEVELING[2]

[1]Department of Geology, Colby College, Waterville, Maine 04901, U.S.A.
[2]Council for Geosciences, Private Bag x112, Silverton, Pretoria, 0001 South Africa
e-mail: ragastal@colby.edu

ABSTRACT: The Lower Triassic Katberg Formation (Beaufort Group, Karoo Supergroup) in South Africa is a fine-grained, arenaceous unit deposited under ephemeral bedload-dominated fluvial conditions and previously interpreted as representing a continuous stratigraphic record. Its genesis was linked directly to the end-Paleozoic extinction event and was considered to exhibit the results of a trend towards aridification. The present study documents the lowermost Katberg Formation exposed at Carlton Heights, Northern Cape Province, to test the aridification hypothesis.

Four lithofacies vary in both vertical and lateral relationships, with feldspathic sandstone dominating the stratigraphy. Pisolith-size nodular conglomerate consists of pedogenically derived carbonate nodules originally precipitated within aridisols, none of which are either exposed or reported from the formation. Rather, the only evidence of extreme aridification is found within channel lag, barform, and overbank deposits marking landscape degradation. Landscape aggradation is characterized by two feldspathic sandstone geometries where (1) medium-bedded, planar bedded, or ripple-laminated sheet sandstone is interpreted as ephemeral sheetflood deposits, and (2) thick-bedded, cross-laminated multi-lateral, lenticular sandstone is interpreted as associated with deeper, sand-bed braided (anabranching) systems. Overbank fines consist of polyphase siltstone paleosols in which bioturbated inceptisols were overprinted by gleysols wherein large pedogenic carbonate nodules precipitated under a high regional water table. Evidence exists for periodic drying in these wet regimes, but no evidence exists for extreme aridity. Hence, the lowermost Katberg Formation superficially exhibits only an aggradational sedimentological record, but significant diastems exist as evidenced by the concentration of aridisol precipitates at the base of each degradational cycle. A model for the Early Triassic in this part of the Karoo Basin is presented wherein this record is interpreted as a function of climate oscillations rather than either episodic uplift in the Cape Fold Belt or any ecosystem response to the end-Permian extinction.

INTRODUCTION

The extinction at the Permian–Triassic boundary (P–Tr), ~ 252.6 million years ago (Mundil et al. 2004), marks the loss of more than 90% of marine taxa and up to 82% of terrestrial vertebrate families (Benton et al. 2004; Ward et al. 2005). On the basis of its rich tetrapod-fossil fauna, the Karoo Basin of South Africa is thought to hold the key to unraveling the nonmarine ecosystem response to the most massive extinction of the Phanerozoic. Over the past two decades, the basin has been the focus of numerous stratigraphical, biostratigraphical, and geochemical studies in an attempt to resolve the position of the terrestrial P–Tr boundary and correlate it with the marine realm (e.g., Smith 1995; Smith and Ward 2001; De Wit et al. 2002; Retallack et al. 2003; De Kock and Kirschvink 2004; Ward et al. 2005; Smith and Botha 2005). The P–Tr event, associated extinction, and recovery of continental ecosystems have become a highly debated topic (Gastaldo et al. 2005; Gastaldo et al. 2009; Tabor et al. 2007; Smith and Botha 2005), with the sedimentological context in which these occurred often obscured by generalities.

According to the most recent interpretation, the end-Permian extinction event, as defined by vertebrate biostratigraphy (Ward et al. 2005), is recorded at the base of the Palingkloof Member, the uppermost subunit of the Balfour Formation (Adelaide Subgroup, Beaufort Group, Karoo Supergroup, Fig. 1). The subsequent biotic recovery is recorded in the Early Triassic rocks of the Palingkloof Member (Balfour Formation) and the overlying arenaceous Katberg Formation (Smith and Botha 2005; Botha and Smith 2006), although Gastaldo et al. (2009) cast doubt on the ability to identify the exact stratigraphic position for the base of the Palingkloof Member in the basin. Biostratigraphic evidence indicates that the Katberg Formation accumulated during the Induan and lower Olenekian stages (Neveling 2004). Gradstein et al. (2004) estimate that this duration spans ~ 3 M, but recent geochronometric data for the Spathian in China has reduced this duration to 2.1 M (Ovtcharova et al. 2006; Galfetti et al. 2007).

A marked sedimentological change in fluvial style is reportedly associated with the P–Tr boundary (Ward et al. 2000; Smith and Botha 2005), with latest Permian (Elandsberg Member) meandering systems replaced, over a 20–40 m interval (Smith and Botha 2005; Ward et al. 2005; Botha and Smith 2006), with braided river systems of the Lower Triassic Katberg Formation. While the P–Tr boundary and Balfour–

---

* Present Address: Mackay School of Earth Sciences and Engineering, Mail Stop 168, Reno, Nevada 89557-0047, U.S.A.
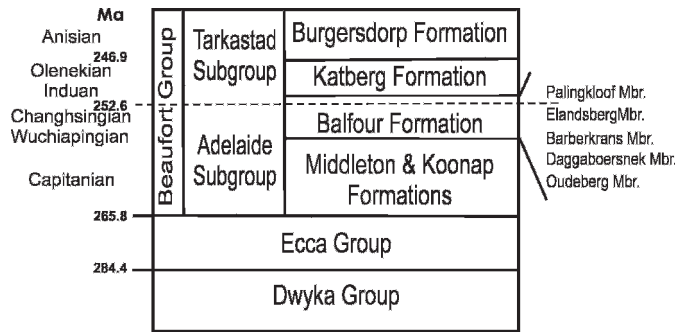
FIG. 1.—Generalized stratigraphy of the Karoo Basin east of 24° E longitude. The age of the P–Tr boundary (dashed line) follows Mundil et al. (2004); the Olenekian–Anisian boundary age follows Galfetti et al. (2007).

Katberg contact are not concordant horizons, this change is considered a direct consequence of the end Paleozoic extinction event (Smith and Ward 2001; Ward et al. 2000; Ward et al. 2005; Smith and Botha 2005). In contrast, earlier researchers (Hiller and Stavrakis 1984; Cole 1992; Catuneanu et al. 1998) postulated that the Katberg Formation was deposited in response to orogenic loading in the Cape Fold Belt, with the base of the formation representing a second-order sequence boundary.

Sedimentological data are an important source for paleo-environmental reconstruction, and based on sedimentary structures, sandstone geometries, and lithofacies associations, the Katberg Formation has been interpreted as accumulating under semiarid conditions (Stavrakis 1980; Hiller and Stavrakis 1984; Smith 1995; Smith and Ward 2001; Botha and Smith 2005). A comprehensive understanding of the Early Triassic is crucial to understanding the environmental framework that impacted the early Triassic terrestrial recovery (Smith and Botha 2005; Botha and Smith 2006). The present study focuses on the lowermost Katberg Formation exposed at Carlton Heights, Northern Cape Province, to reassess earlier climatic interpretations for the genesis of these rocks and the reported continuous nature of sedimentation during this time interval (e.g., Smith and Ward 2001).

GEOLOGY OF THE KAROO BASIN

The development of the Karoo Basin commenced in the Late Carboniferous, first as a passive margin and then a retroarc foreland basin that formed as a result from the collision of the paleo-Pacific plate with the Gondwanan plate (Smith 1995). The impact of plate convergence resulted in the emplacement of the Cape Fold Belt onto the edge of the basin and subsequent sediment sourcing from that provenance (Catuneanu et al. 1998). The entire stratigraphic section, spanning the Carboniferous to the Jurassic and attaining a maximum thickness of 12 km, is known as the Karoo Supergroup (Johnson et al. 1997). As the basin evolved, siliciclastics accumulated under a variety of conditions, starting with glacial sedimentation of the Dwyka Group at the base, followed by deep-water and coastal deposits of the Ecca Group (Fig. 1). This was followed by fluvial deposition that formed the rocks of the Beaufort Group and the overlying Molteno and Elliot formations, before continued aridification resulted in sediment accumulation under eolian conditions, the Clarens Formation (Johnson et al. 1997).

The Beaufort Group, considered to be the first fully continental sequence in the Karoo Supergroup, also is its largest unit in terms of thickness and spatial distribution. Clastic input and discharge were derived mainly from the Cape Fold Belt to the south. In the lower part, the Koonap, Middleton, and Balfour formations (Adelaide Subgroup; Fig. 1) are interpreted as fluvial–lacustrine depositional systems in which wet floodplains with high water tables were maintained under a relatively humid environment (Smith et al. 1993; Catuneanu and Bowker 2001).
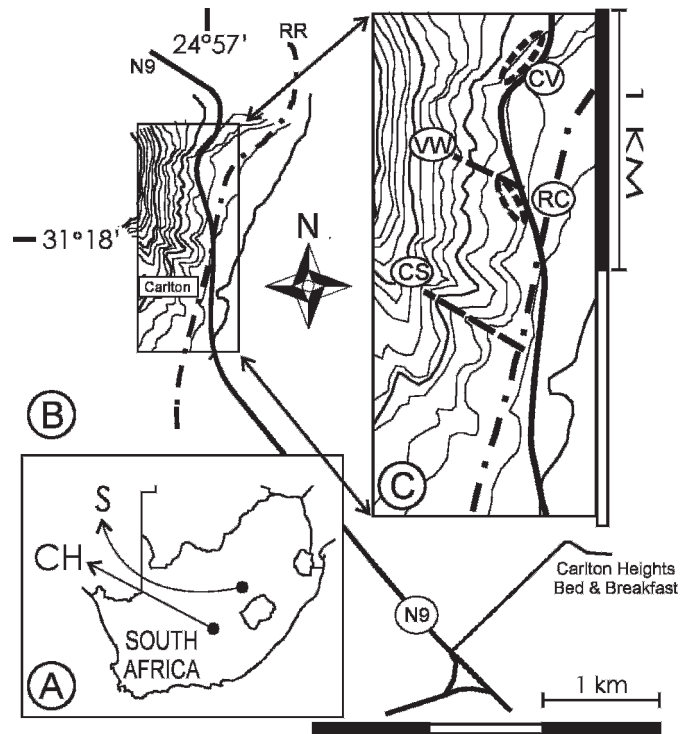

FIG. 2.—Locality map of Katberg Formation at Carlton Heights. A) Inset map of South Africa with localities at Carlton Heights (CH) and Senekal (S) noted. B) The N9 highway runs SE to NW and is adjacent to the Carlton Heights railway (RR). Study area within small rectangle is enlarged in part C; scale in km. C) Measured sections in the present study include: CS = Caution Sign donga section (31.29678° S, 24.95108° E); VW = VW donga section (31.29328° S, 24.95155° E) with adjacent road cut = RC; and CV = outcrop that parallels the highway near the top of the incline (31.29228° S, 24.95152° E). Contour Interval = 10 m; Scale in km.

Fluvial systems of the Upper Permian Balfour Formation and its regional equivalents consist of meandering-channel architectures (Hiller and Stavrakis 1984; Stear 1985; Smith 1987; Ward et al. 2000) with individual sandstone intervals reported to be < 10 m thick (Catuneanu and Elango 2001). The overlying Tarkastad Subgroup, which has a more restricted spatial distribution and crops out only to the east of 24° E, is subdivided into the arenaceous Katberg and argillaceous Burgersdorp formations (Johnson et al. 1997). A low-sinuosity fluvial system is accepted for the emplacement of the former, while the latter exhibits features of meandering fluvial systems, albeit of a lower sinuosity than recorded in the Balfour Formation (Hiller and Stavrakis 1984; Smith 1995; Ward et al. 2000).

Steiner et al. (2003) described the P–Tr boundary as occurring within the Katberg Formation, but the majority of workers place this horizon some stratigraphic distance (i.e., 20–40 m) below (Ward et al. 2005; Smith and Botha 2006). In more proximal southern exposures, the boundary is placed between the Elandsberg (P) and Palingkloof (Tr) Members (Balfour Formation), whereas it is placed at the base of the Harrismith (Tr) Member of the Normandien Formation in the north (Johnson et al. 1997). The Late Permian to Middle Triassic interval in the south (Balfour, Katberg, and Burgersdorp formations) is interpreted to represent a fairly continuous record of sedimentation (Smith 1995; Ward et al. 2000; Smith and Ward 2001; Neveling 2004) with no significant stratigraphic breaks. In contrast, the interval is more attenuated in the distal areas to the north, where it contains significant chronostratigraphic breaks. For example, Hancox et al. (2002) demonstrated that the entire Palingkloof Member was removed by erosion prior to the deposition of the overlying Katberg Formation in the northwestern exposures near Senekal (Fig. 2A), while

Neveling (2004) postulated the lower Katberg Formation to be absent from the northern exposures.

Overview of the Katberg Formation

Very little detailed research has been dedicated to the sedimentology of the Katberg Formation, and the majority of reports published over the last decade, in which the sandstones of the lower Katberg Formation are discussed, provide little more than the most basic characterization of the unit. Instead, the primary focus has been on vertebrate paleontology (e.g., Smith and Ward 2001; Smith and Botha 2006) and geochemistry (MacLeod et al. 2000; Tabor et al. 2007) in relation to the P–Tr boundary event. With the exception of Groenewald (1996), who traced the formation throughout the basin, all studies have been restricted stratigraphically and geographically.

Du Toit (1917) first recognized the Katberg Formation as an arenaceous interval in the Beaufort Group rocks, exposed in the Eastern Cape Province, that he mapped as the "Middle Beaufort Beds." Marais and Johnson (1965) and Johnson (1966) proposed the name "Katberg Sandstones" for this interval, the nomenclature of which subsequently was modified to the Katberg Formation (Johnson 1976; S.A.C.S. 1980). Traditionally, it is defined as an arenaceous or predominantly arenaceous unit (Johnson 1976; S.A.C.S. 1980), while more recent workers (Smith 1995; Groenewald 1996) described it as consisting of sandstones with subordinate, thin (2–10 m) red and greenish gray mudstone beds.

The greenish gray, light olive gray, and less commonly pinkish gray (Johnson 1976; Hiller and Stavrakis 1984; Groenewald 1996) sandstones are predominantly fine to medium grained (Hiller and Stavrakis 1984; Smith 1995; Groenewald 1996), but coarse, pebbly sandstone also is documented in the coastal Katberg exposures at East London, situated 100 km proximal of the main outcrop belt (Hiller and Stavrakis 1980). Similar coarse grain sizes were documented in the distal exposures in the northern Free State, but these are interpreted to represent input from a local sediment source north of the basin (Groenewald 1989; Hancox et al. 2002).

Horizontal bedding is the dominant sedimentary structure encountered, although trough-, planar-, and ripple-cross bedding also is common (Hiller and Stavrakis 1984; Smith 1995; Groenewald 1996; Neveling 2004). Sandstone architecture universally is described as consisting of thin (< 1.5 m), tabular sheets that are individually bounded by erosional and sharp surfaces (Hiller and Stavrakis 1984; Smith 1995; Groenewald 1996; Ward et al. 2000). Many authors describe these sheet sandstones as laterally extensive and vertically stacked, forming multiple stories of tabular sandstone, 5–10 m thick (Ward et al. 2000; Smith and Ward 2001; Steiner et al. 2003). The presence of intraformational mud pebbles and pedogenic carbonate clasts has been used by Johnson (1976), Smith and Ward (2001), Smith and Botha (2005), Abdala et al. (2006), and Botha and Smith (2006) as the criterion to delineate the first appearance of the Katberg Formation in the Karoo Basin. A more frequent occurrence of desiccation cracks and sand-filled mudcracks also has been used to distinguish these sandstone bodies from those of the Permian (Steiner et al. 2003).

A braided-fluvial model was proposed first for the Katberg Formation by Johnson (1976) based on vertical lithofacies relationships. By incorporating sandstone geometries and more detailed sedimentological data, Hiller and Stavrakis (1984) and Smith (1995) further refined this model to consist of wide and shallow braided channels set in an ephemeral environment developed under semiarid climatic conditions. In addition, Groenewald (1996) also recognized subordinate deposits representing floodplain, playa lake, and lacustrine environments. This low-sinuosity fluvial model has been accepted, virtually unchanged, by subsequent authors (Ward et al. 2000; Smith and Ward 2001; Hancox et al. 2002; Retallack et al. 2003; Steiner et al. 2003).

MATERIALS AND METHODS

The base of the Katberg Formation, attaining a thickness of > 300 m in the vicinity of the study area (Groenewald 1996), is well exposed along the N9 highway near the Carlton Heights railway stop (31.29415° S, 24.95057° E WGS84 Meridian), Northern Cape Province (Fig. 2). Outcrops here consist of resistant sandstone benches up to 4 m thick with intervening, slope-forming siltstone. Roadcuts provide the best examination of mesoscale outcrop features, while dongas (erosional gullies) provide the most continuous exposures over long vertical sections. Much of the area is vegetated sparsely; however, the ground surface is covered with rock debris, somewhat limiting exposure. This cover feature, along with minimal soil development, allowed documentation and correlation of three vertical sections over a horizontal distance of 1.15 km.

Two stratigraphic columns, each > 100 thick were characterized on a sub-meter scale (Fig. 2C, CS and VW) using standard field methods and a Jacob's staff with leveling eyepiece; architectural elements and lateral facies relationships were identified using photomosaics, and bounding surfaces were traced by foot in the field. Six short, detailed sections were logged on a centimeter scale in the lower roadcut exposures, one section was studied along a curving roadcut to document a sand-dominated section (Fig. 2C, CV), and five sections were investigated along a longer roadcut exposure (trending 040°) and an adjacent donga (trending 006°) to document lateral variability (Fig. 2C, RC). Hence, two different orientations of correlative beds were examined.

The Caution Sign donga section was measured southwest of the main N9 roadcut at Carlton Heights (31.29678° S 24.95108° E WGS84 Meridian; Fig. 2C, CS). The base begins at the road level of the N9 near the point where the road bridge crosses the railway line entrance to the Carlton Heights railway stop, with a total of 102 m of vertical section logged. Thirty beds, grouped into 12 sandstone-dominated sets, were recognized in the CS section (Fig. 3A).

An 115 m section (Fig. 3B) was measured in the VW donga (so-called after a motor wreck encountered here) immediately to the north of the main roadcut exposure (Fig. 2C, VW). This continuous section encompasses the uppermost Palingkloof Member and the basal Katberg Formation, and is the same as that documented by earlier workers (Retallack et al. 2003; Steiner et al. 2003; Gastaldo et al. 2005; Tabor et al. 2007) in attempts to constrain the P–Tr boundary. The base is positioned just below the point of changeover from silt-dominated to sand-dominated facies, characteristic of the Katberg–Palingkloof contact. This occurs at the base of the sandstone bench that crops out in the donga immediately below the N9 (31.29328° S 24.95155° E WGS84 Meridian; Fig. 2C, VW). Although the VW donga section exposes the best vertical outcrop within several erosional cuts that exist up the side of the butte, a continuous measured section is not possible here alone because of overburden (e.g., rockfall and other donga infill). Hence, adjacent dongas were correlated by foot and measured to complete the 115 m of section above the resistant sandstone benches (Fig. 4).

A third outcrop to the northeast of the VW donga along a curve in the road (31.29228° S 24.95152° E WGS84 Meridian; Fig. 2C, CV) exposes > 4 m of stacked sandstone with little intercalated siltstone (Fig. 3C). The third sandstone unit of the lower Katberg Formation, which is exposed as the third bench along the N9 highway (Fig. 2C, RC), was detailed to document lateral variation in lithofacies distribution and architecture (Fig. 4, SS3).

Lithofacies are defined based on grain size, primary and secondary sedimentary structures, and composition. Due to the fine-grained nature of all rocks, representative hand samples were collected throughout the area for further characterization of composition and microstructure following laboratory examination. Polished thin sections of each field-identified lithofacies were studied using light microscopy and scanning
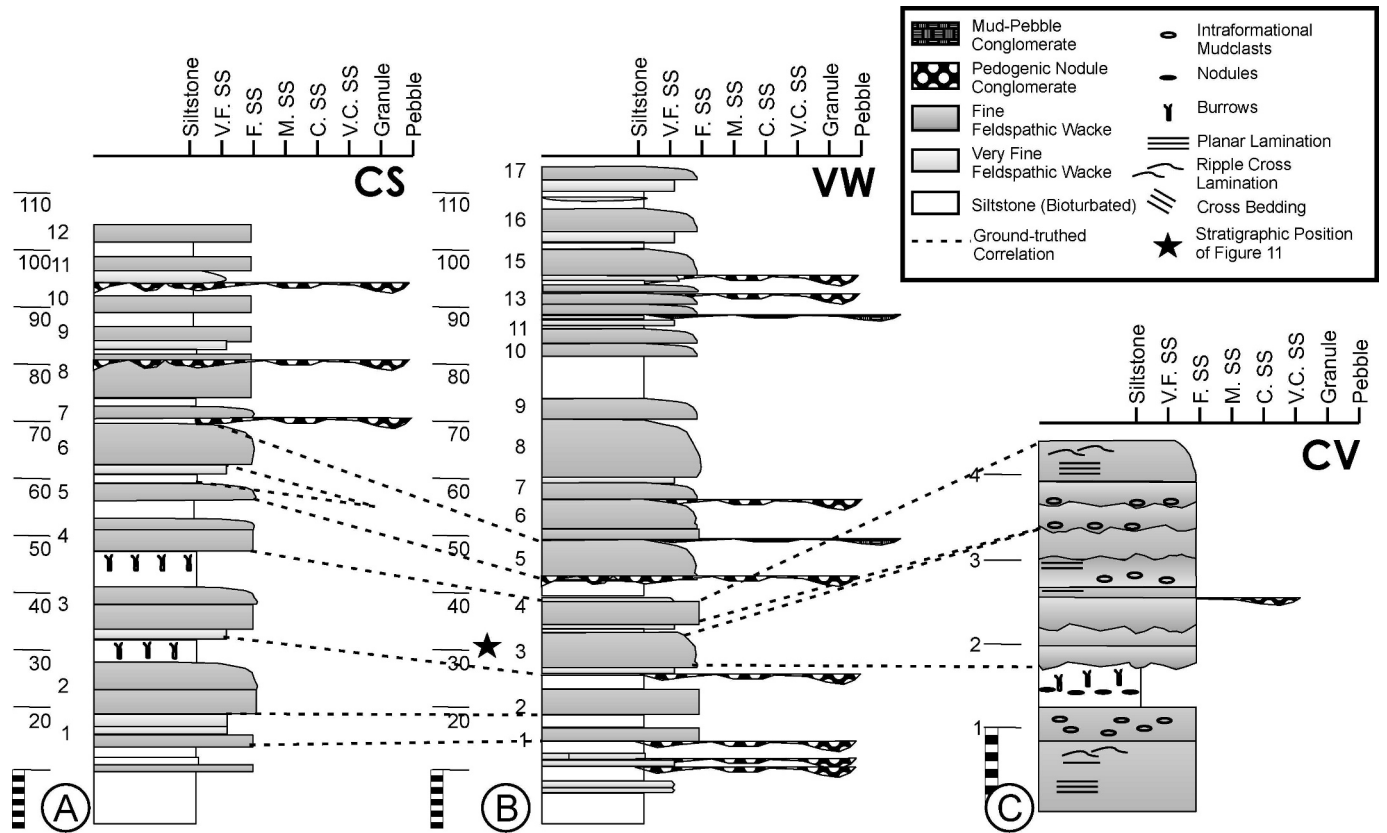
FIG. 3.—Measured stratigraphic columns of the Katberg Formation. See Figure 2 for locations. **A)** Caution Sign (CS) donga section—a continuous section beginning at a caution sign logged on a meter scale and correlated laterally where possible. Twelve [12] sandstone bodies, numbered along the stratigraphic column, were encountered. Scale in meters. **B)** VW donga section—this is a stratigraphically higher section of the donga often used to study the P–Tr boundary. Section was logged on a meter scale and correlated laterally where possible. Seventeen [17] sandstone bodies, numbered along the stratigraphic column, were encountered. Scale in meters. **C)** A short section recorded along a bend (CV) in the N9 highway documented on a decimeter scale. The stratigraphic position of Figure 11 is indicated by a star. Correlations are based on bounding surfaces of resistant sandstones walked across the outcrop. Scale in A and B = 10 m; scale in C = 1 m.

election microscopy with EDAX Genesis software (Colby College SEM facility). Powdered rock samples were analyzed using a Rigaku D-Max B two-axis X-ray diffractometer and Jade MDI 7 software. No samples were hydrated to facilitate identification of clay minerals or differentiate clays from mica platelets identified in thin section. Hence, the term muscovite-like clay minerals is used herein as an all-inclusive category that comprises most of the clay fraction as well as some lithic fragments. Feldspar clasts were identified in thin section and through X-ray diffraction (XRD) analyses but were not further subdivided. XRD data are given in weight %, and point-count data are based on a minimum of 300 points per sample.

Architectural elements and stacking patterns were studied further by walking out beds in the field, and tracing them manually and digitally on photomosaics. Terminology for bounding surfaces and architectural elements follows Miall (1996).

LITHOFACIES AND INTERPRETATIONS

The Katberg Formation is identified by the appearance of thick, fine-grained sandstone bodies that feature pisolith-size, carbonate-nodule, channel-lag accumulations (Johnson 1976; Smith and Ward 2001; Smith and Botha 2005; Botha and Smith 2006). These lags are distinguishable in

FIG. 4.—Photograph of the first three sandstone units (SS1, SS2, SS3) in the Katberg Formation exposed along the N9 roadcut. See Figure 11 for details and scale of SS #3.

the field by brownish-white concretions organized into lenticular geometries (0.1–0.2 m depth; > 2 m width) above erosional contacts, and are overlain by graywackes that occur as planar-laminated and ripple cross-laminated, very fine-grained sheet sandstone interbedded with centimeter-scale siltstone. Sharp, irregular erosional contacts characterize a transition into tabular trough cross-bedded sandstone lenses in stacked packages and associated mud-pebble conglomerate. These units fine upward into heavily bioturbated siltstone in which *in situ* carbonate nodules and isolated lenses of very fine-grained sandstone occur. Overall, these medium- (0.1–0.3 m) to thick- (0.3–1.0 m) bedded siltstone units have tabular geometries, but may appear lenticular due to the impact of laterally extensive erosional surfaces (see below).

Nodular Conglomerate

This coarsest lithofacies is composed of small carbonate nodules, mud clasts, and bone fragments set in a matrix of very fine-grained sandstone and coarse siltstone (Fig. 5). It is pale olive (10Y6/2) and weathers moderate yellowish brown (10YR 5/4). Nodules effervesce readily when exposed to dilute HCl and vary in diameter from 0.5 to 3 cm. Nodules range from subrounded rods to well-rounded spheres in shape, although some appear amorphous (Fig. 5B). Compositionally, they are commonly calcite spar, although micritic nodules also are present. The nodules show a range of internal structures, from concentric mud coatings around a crystalline core to crystallized rinds around a mud core.

Nodular conglomerates are exposed mainly as thin (0.03–0.1 m) to medium (0.1–0.3 m) thick lenses with undulatory bases that are in sharp erosional contact with underlying siltstone (Fig. 5A) and/or sandstone. Lenses are planar or trough cross-bedded and fine upward into, or are separated by abrupt contacts from, overlying very fine-grained sheet sandstone. Isolated thin conglomerate lenses occasionally are found in siltstone-dominated intervals that may be associated with thin, lenticular or tabular feldspathic graywacke.

Thick lenses (30–100 cm) of cross-bedded nodular conglomerate incise up to 3 m into the underlying sandstone and siltstone (Fig. 6), and are associated with thick cross-bedded fine-grained feldspathic graywacke. Individually these thick lenses pinch out over a distance of meters, but when the bounding surface is traced laterally over several hundred meters, smaller, medium thick (10–30 cm) conglomerate lenses were recorded at the base of the same overlying sandstone body.

Interpretation.—Carbonate-nodule conglomerate is found in channel-lag, barform, and overbank deposits. Stable-isotope values of micrite cements in these nodules indicate carbonate precipitation was in atmospheric equilibrium (Tabor et al. 2007). As such, their concentration above erosional contacts within fluvial systems represents the remnants of phreatic zones of aridisols or calcisols that developed across the Early Triassic landscape. Retallack et al. (2003) identified calcic xerosols (Karie and Kuta) based on the presence of carbonate nodules in reddish-brown siltstone, but the nodules in these soil types are not of pisolith size. Rather, nodules in Karie and Kuta paleosols are those identified in the siltstone lithofacies, and they precipitated under wetland conditions (Tabor et al. 2007; Gastaldo and Rolerson 2008). Hence, aridisols have not been verified, to date, anywhere else in the basin at this stratigraphic horizon (Neveling 2004), and are represented only in these lag, barform, and overbank deposits. Smith (1993) noted calcite pseudomorphs after gypsum roses in siltstones of the Upper Permian Hoedemaker Member, restricted to the southwestern part of the basin. But, the aridisol (or calcisol) residuum in the Katberg Formation represents the only evidence of extreme aridity (Sellwood and Price 1994) and a minimal rainfall regime (Cecil and DuLong 2003). Their restricted occurrence in channel-lag and overbank deposits indicates that these soils subsequently were scavenged during landscape degradation (Allen 1974, 1986).

Fine-Grained Feldspathic Wacke

Pale olive (10Y6/2), immature, feldspathic wacke consisting of fine-grained, subangular grains, is differentiated in the field by thicker bed structures, coarser grain size, and lower matrix content. Mineralogical composition based on optical point counts (Fig. 7A), scanning electron microscopy (Fig. 7B), and XRD bulk composition is shown in Table 1. Cement is dominantly siliceous with a minor carbonate component.

Beds of feldspathic wacke are arranged in 1–3 m thick, lenticular geometries with extensively scoured bases. Basal incisions into underlying lithofacies are generally > 0.5 m, with maximum observed depths in the study area of up to 3 m. Some lenticular bodies are *en echelon* stacked (multilateral channel geometry *sensu* Gibling 2006), but most show a succession-dominated vertical stacking pattern. Downstream accretion bars with trough cross-bedding are the dominant architectural elements from which paleocurrent data were collected (Fig. 8). A mean paleocurrent direction of 340° is found when cross-bed orientations are plotted on a rose diagram; a mean direction of 327° is calculated when parting-lineation data are included (Fig. 8B). Paleocurrent data taken from flute-cast orientations indicate that flow was to the north. Exposed megaforms display wavelengths that vary from 18 m to 50 m, with amplitudes of 1–2 m, respectively. Sharp contacts separate individual units with flute casts preserved on their bases. Mud pebbles often are concentrated along bed contacts, and occur dispersed throughout beds or as mud-pebble conglomerate in lenses up to 0.5 m thick and 30 m in length. These may show crude low-angle trough cross-bedding. Individual mud pebbles may be up to 3 cm in diameter and are similar to other siltstone lithofacies in color and grain size, differing only in their more rubbly surface texture. Contacts become more gradational, and incisions become shallower and less pervasive, toward the tops of sandstone units. While individual bedsets are typically trough cross-bedded. with thicknesses up to 50 cm, other structures include low-angle planar cross-lamination as millimeter-scale beds in bedsets 10–20 cm thick, and ripple cross-laminated bedsets. The latter are more common toward the tops of sandstone-dominated units, which exhibit fining-upward trends.

Interpretation.—The fine-grained feldspathic wacke, organized into stacked lenticular geometries, is interpreted as deposits of downstream-accretion macroforms and sandy barforms (cf. Miall 1996). Mud clast conglomerate interbedded with the sandstone consist of rip-up clasts of interfluvial paleosols, and are interpreted as filled hollows where they occur in thick scoop-shaped lenses in fine-grained feldspathic wacke. To date, no evidence for bedload transport of sand-size pedogenic aggregates (e.g., Rust and Nanson 1989; Wright and Marriott 2007) has been found in thin sections. The architectural elements are characteristic of a high-energy, multi-lateral (Gibling 2006), sand-bedload-dominated braided system (Miall 1996).

Very Fine-Grained Feldspathic Wacke

The other sandstone lithofacies is a light olive gray (5Y6/2) immature, feldspathic wacke consisting of very fine subangular grains. It is classified as a silty wacke based on point count and XRD bulk-composition data. The large siltstone fraction, composed predominantly of muscovite-like clay minerals, accounts for the discrepancy in the results from microscopy and XRD analyses (Table 1). Cements are siliceous with occasional carbonate overgrowths identified in thin section.

This lithofacies is exposed as medium thick (0.05–0.3 m) laminated sheets in sharp contact with underlying and overlying units. Beds are laterally extensive, traced over distances of > 75 m, and form stacked packages up to 2 m thick. Basal scouring into the underlying units is < 0.5 m deep. Planar cross-bedding and ripple cross-lamination (Fig. 9A) are common, with occasional centimeter-scale, shallow desiccation cracks on upper bed surfaces (Fig. 9B). Ripple wavelengths
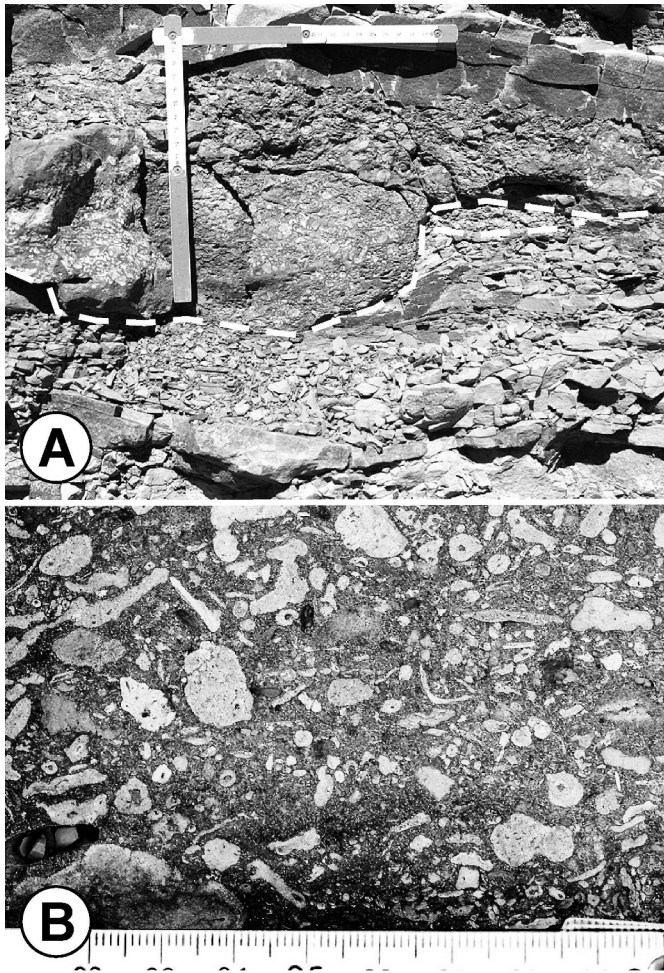
FIG. 5.— Nodular pebble conglomerate. **A)** Outcrop exposure where nodular pebble conglomerate eroded into underlying siltstone. White dotted line shows the sharp erosional contact between lithologies and the angular nature of the contact; scale in dm. **B)** Photograph of conglomerate showing range in size and shape of calcitic nodules. Scale in mm.

are typically in the 10–30 cm range, with amplitudes of ~ 1 cm (Fig. 9C). These are asymmetrical with the lee side generally to the north. Desiccation features occur on the upper surfaces of lenticular barforms and range from 2–10 cm in thickness, but are not ubiquitous along bed contacts and may disappear over a distance of a few meters. Closer analysis revealed these structures to be restricted generally to barform crests, but absent from the rippled surfaces near and within troughs. Laminated siltstone and mudstone drapes occur interbedded with laminated sheet sandstones.

Interpretation.—Laminated sheet sandstone that occurs throughout many basal units, the most common occurrence of the very-fine grained feldspathic wacke, are best interpreted as flashy, ephemeral sheetflood deposits (cf. Miall 1996). These macroforms best conform to sandstone geometries, sedimentary structures, and depositional environments traditionally described for the Katberg Formation (Hiller and Stavrakis 1984; Smith 1995; Ward et al. 2000).

Bioturbated Siltstone

The fourth lithofacies is a bioturbated siltstone that is pale olive (10Y5/2) mottled with brown gray (5YR3/2). A high degree of color variation

occurs, and the color pattern and degree of mottling is equally variable depending on weathering, lighting, and other characteristics of a given exposure. Those recorded herein are the best interpretation of pure end-member colors in the mottled units. Internally, this lithofacies has a massive appearance and is interbedded with other lithologies, such as centimeter-scale very fine-grained feldspathic wacke lenses and nodular conglomerate. XRD analysis shows a predominance of muscovite-like clay minerals (Table 1), while some samples react mildly with HCl, indicating the presence of carbonate cement. Horizons of sandstone-filled desiccation cracks, up to 12 cm deep, with a maximum upper and lower widths of ~ 6 cm and ~ 2 cm, respectively, occur. These structures are common where bounded by sandstone lenses or interbedded sandstone and siltstone units (Fig. 10A). In these instances, mudcrack depth is limited by the thickness of individual siltstone units. Mud-cracked horizons in siltstone units, as well as isolated lenses of sandstone and nodular conglomerate, can be traced up to 20 m along horizontal exposures (Fig. 11).

Siltstone units are burrowed at densities of up to $12/m^2$ of outcrop, and bioturbation generally is restricted to the upper 0.5 m of most beds. Burrows average 1–2 cm in diameter and decimeter scale in length when partially exposed. They are inclined (Fig. 10B), sinusoidal in geometry, and may preserve an expanded chamber at the base (Gastaldo and Rolerson 2008). A three-part hierarchy of scratch ornamentation marks the surfaces of the burrow, and fill is most commonly siltstone, although some sandstone fill also is present and dependent upon the relationship, in some cases, with overlying lithologies. Gastaldo and Rolerson (2008) have assigned these burrows to a new ichnotaxon, *Katbergia carltonichnus*.

Carbonate-nodule horizons occur in thicker siltstone intervals. These elliptical nodules differ from the pisolith-size nodular conglomerate, found in channel lags, by exhibiting a maximum diameter of 60 cm and having a relatively indistinct surface texture. All nodules occur along one or two discrete horizons per siltstone interval (Fig. 10C). Nodule horizons may overlap the lowermost decimeter of the *Katbergia*-burrowed interval or occur below the termination of burrow penetration. Nodules generally are discrete from burrows, although burrows have been found that crosscut nodules (Fig. 10D). Density is approximately $10/m^2$ of exposure, and stable-isotope data indicate that carbonate cement contained within burrows, entombing siltstone, and nodules are secondary and early diagenetic (Tabor et al. 2007; Gastaldo and Rolerson 2008).

Interpretation.—The siltstone facies represent overbank deposits, and where *Katbergia* bioturbation is preserved, this biological activity indicates invertebrate colonization of interfluvial paleosols (Gastaldo and Rolerson 2008). The cylindrical burrows were hollow, with a terminal living chamber that existed above the water table. Hence, when bioturbation was characteristic of a siltstone interval, seasonal but moist conditions prevailed (Hasiotis 2000; Gastaldo and Rolerson 2008). The presence of calcitic nodules organized at discrete horizons indicates that the concretions formed after the burrow-hosted interval became uninhabitable. This is evidenced by the crosscutting relationships of the burrows and nodules (Fig. 10D) as well as the isotopic nature of the radiaxial calcite (Tabor et al. 2007; Gastaldo and Rolerson 2008). Nodule horizons mark an increasing water table, inasmuch as the $\delta^{13}C$ data indicate formation under saturated conditions isolated from input of atmospheric CO_2 (Tabor et al. 2007). It must be noted that not all siltstone, carbonate-nodule-bearing intervals preserve *Katbergia*, although the geochemical signature of a closed, wetland system prevails in these instances (Tabor et al. 2007). These recent data conflict with previous interpretations wherein the bioturbated paleosol (Patha), along with other nodule-bearing paleosols (Kuta and Karie), are considered to represent dry woodland conditions (Retallack et al. 2003). And, the depth
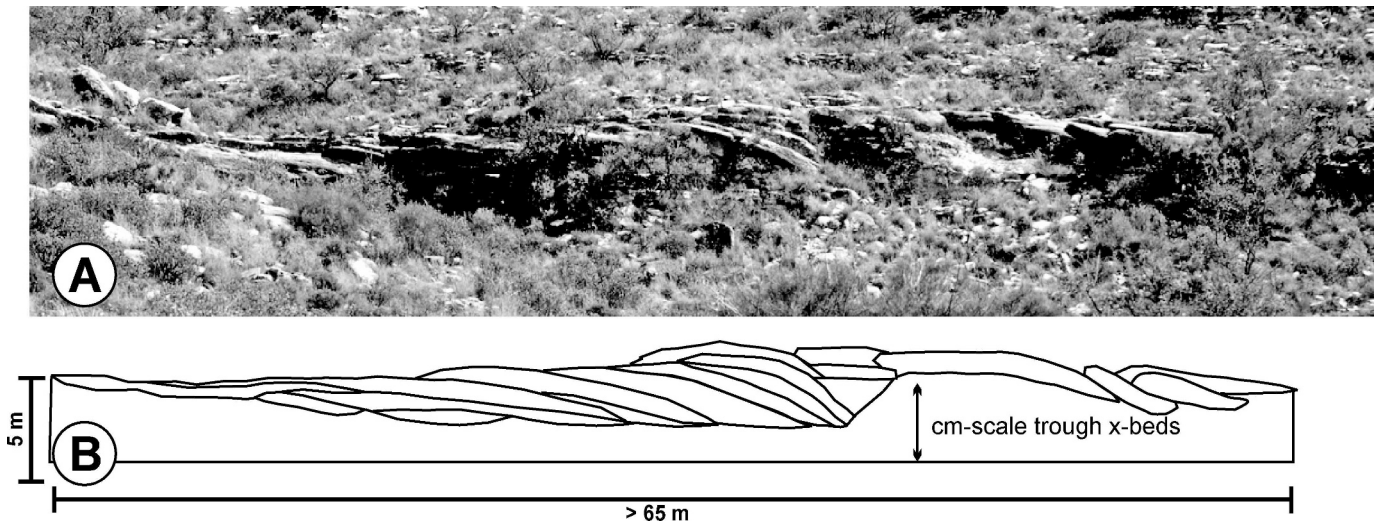
FIG. 6.—Cross-bedded nodular pebble conglomerate just to the northeast of the VW donga. **A)** Landscape degradation event marked by a 3 m incision into underlying centimeter-scale, trough cross-bedded very fine-grained feldspathic lithic wacke. Nodular conglomerate occurs in lateral accretionary beds up to 50 cm in thickness and 10 m in width. **B)** Line drawing of photomosaic taken from the sandstone benches adjacent to the N9 highway showing the character of the incision and stacked conglomerate geometries.

to calcic profile is considered original soil fabric and is used to estimate early Triassic paleoprecipitation patterns (Retallack et al. 2003). The paleosols at Carlton Heights, though, are polyphase in their development (Gastaldo and Rolerson 2008) wherein bioturbated inceptisols were overprinted by gleysols, and large pedogenic carbonate nodules precipitated under a high regional water table (Tabor et al. 2007).

LATERAL FACIES RELATIONSHIPS

Vertical and lateral lithofacies relationships vary dramatically over small spatial distances. Third-order bounding surfaces traced across photomosaics of the roadcut reveal the geometries of the beds, and similar geometries occur throughout the remainder of measured sections. The pattern exhibited in the studied sequence generally mirrors that of the sandstone units on the exposed benches adjacent to the N9, and will serve as a model for the lower Katberg Formation (Figs. 11, 12). The focus will be on the third bench (Fig. 4, SS3).

Nodular conglomerate lenses occur across the exposure, but the number of these varies between individual short stratigraphic sections (Fig. 11). These lenses may be up to 25 cm thick and are interbedded with sheets of very-fine grained feldspathic wacke to form bedsets that are up to 2 m thick in the uppermost sandstone bench. Significant lateral variation exists in the nodular conglomerate. For instance, while it is prominent in the northeastern edge of the outcrop (Fig. 11D) and continues into the donga section (Fig. 11E), it pinches out to the southwest (Fig. 11A). Individual beds bounded by third-order surfaces pinch and swell in an irregular manner across the outcrop (Fig. 12). Most of the vertical and lateral variability in this lithofacies association is the result of third-order surface incision, with maximum incision of 3 m documented in the southwestern edge of the outcrop (Fig. 11A).

Lenticular bodies of fine-grained feldspathic graywacke and mud-pebble conglomerate overlie these bounding surfaces. Sandstone bodies are stacked in an offset (multilateral) pattern to the northeast, with mud-pebble conglomerate isolated within troughs of sandstone bodies (Fig. 12). Individual sandstone beds are constricted laterally and pinch out from thicknesses of > 1 m over exposed lateral distances as little as 10 m. Variation within the *Katbergia*-bearing paleosols includes the presence of thin sandstone lenses, which pinch out over lateral distances

of < 10 m (Fig. 3, SS3), and dispersed *in situ* carbonate nodules usually are found along a single horizon. Isolated deep-penetrating mudcracks (at least 10 cm) occur sporadically beneath thin sandstone lenses, and may reach depths of 12 cm (Fig. 11C, D).

The patterns identified in the upper bench also occur in the two lower benches of the N9 roadcut. A sharp, irregular contact separates *Katbergia*-bioturbated paleosols from the overlying fine-grained feld-spathic wacke that forms the basal sandstone bench (SS1, Fig. 4). The bench is made up of stacked, thick to very thick (maximum thickness of 2.5 m) fine wacke lenses that are bound by sharp contacts and are interbedded with thin lenses of mud-pebble conglomerate. An erosional third-order bounding surface within this sequence, which directly overlies the siltstone in the southwest, cuts out at least 2 m of sandstone over a lateral distance of 100 m. The bounding surface is overlain by a very thick lenticular sandstone, with two lenticular sandstones offset on either side, one to the northeast and to the southwest. A sharp, undulatory upper contact separates it from 1–2 m of *Katbergia*-bioturbated paleosol that thins to the northeast of the exposure.

Smaller lenticular bodies of fine-grained feldspathic wacke drape the basal bounding surface of the second bench (SS2, Fig. 4). These sandstone bodies commonly are isolated, medium bedded, < 5 m in lateral extent, and overlain by mud-pebble conglomerate and/or thick lenticular sandstone. Mud-pebble conglomerate occurs across the outcrop for ~ 50 m, and is bounded above and below by thick lenticular sandstone. These sandstone bodies amalgamate to the northwest, leaving no trace of the mud-pebble conglomerate. A rare siltstone lens is preserved in this sequence of stacked lenticular sandstone and contains a horizon of deep mudcracks (at least 10 cm in depth, Fig. 10A). The upper contact of the sandstone interval is sharp and undulatory, with ripple marks and shallow desiccation cracks preserved sporadically.

Macroscale analysis indicates that extensive lateral variation occurs throughout the 100 m of vertical section studied. Incisions similar to the one exposed in the uppermost roadcut bench (Figs. 11A, 12) are pervasive. Two sandstone-dominated sets consisting of fine-grained feldspathic wacke are separated by 4 m of *Katbergia*-bioturbated paleosol and 3 m of very fine-grained wacke in Caution Sign Donga (Fig. 3A, SS3-4) but amalgamate to the north, separated only by < 1 m of *Katbergia*-bioturbated paleosol in the VW donga (Fig. 3B). This results in a
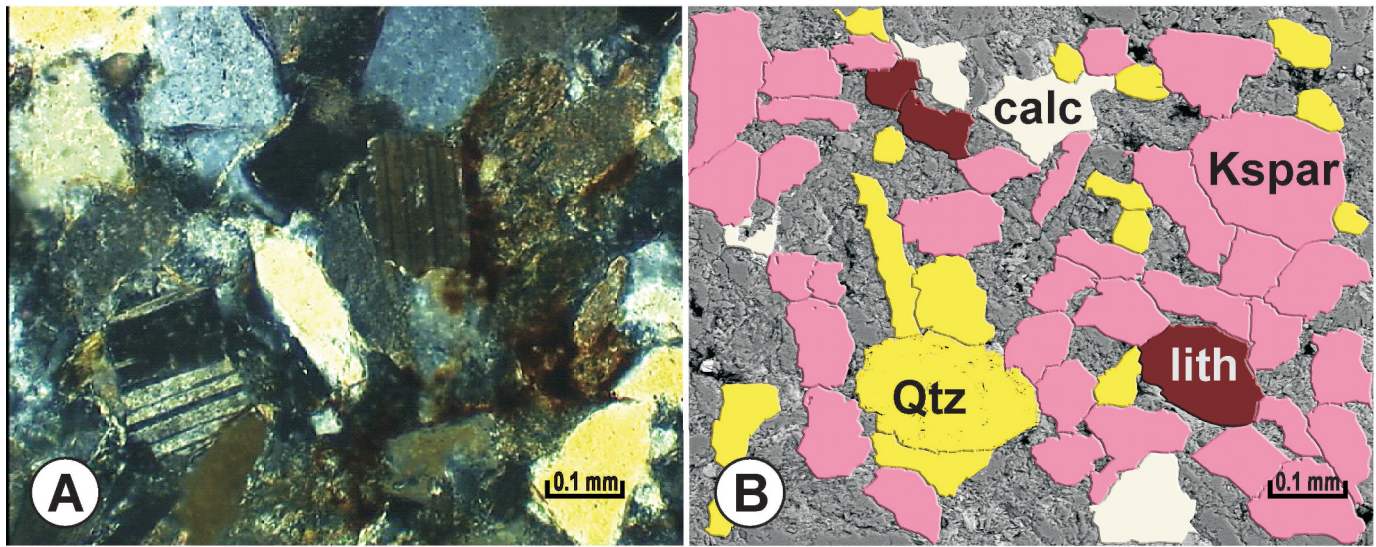
FIG. 7.—Fine-grained wacke. **A)** Photomicrograph of fine-grained feldspathic wacke from channel-form geometry (see Fig. 12). Twinning and cleavage planes are visible in feldspars. **B)** Backscattered electron-image trace based on chemical composition of fine-grained wacke. Images are from the same thin section but are not the same field of view. Qtz = quartz, Kspar = feldspar, calc = calcite, lith = lithic clast. scale = 0.1 mm.

seemingly continuous series of lenticular, stacked beds of fine-grained feldspathic wacke in exposures farther to the north (Fig. 2, CV). Similar amalgamations of sandstone are seen elsewhere, for example, in units 5 and 6 between Caution Sign and VW dongas (Fig. 3A, B). Northeast of the VW Donga, a nodular conglomerate-filled incision occurs, the base of which is downcut 3 m into the underlying very-fine grained feldspathic wacke (Fig. 6). When traced laterally, this unit pinches out over a distance of < 200 m and is overlain by fine-grained feldspathic wacke along third-order bounding surfaces. Nodular conglomerate reappears numerous times in medium (10–30 cm) thick, laterally isolated lenses along the same bounding surface. Lithofacies relationships were not traced out laterally above sandstone unit 6, but similar amalgamations occur throughout the basal-most Katberg Formation on the basis of photomosaic analysis.

STRATIGRAPHIC FACIES RELATIONSHIPS

Recurrent deep incisions and resultant erosional contacts in the section result in a highly variable sequence at Carlton Heights. The most common and resistant succession consists of vertically stacked units of fine-grained feldspathic wacke separated by mud-pebble conglomerate. The intervening *Katbergia*-bioturbated paleosol is sporadically present depending upon the degree of sandstone incision. Basal nodular conglomerate and very fine-grained sandstone sheets occur in some of the siltstone units but are exposed only in areas where incision has not been pervasive. These two

lithofacies do not always co-occur, and isolated very fine sandstone sheets and lenses, or lenticular nodular conglomerates, appear within thicker *Katbergia*-bearing and non-*Katbergia*-bearing siltstone intervals.

Complete genetic sequences are rare in the study area as a result of the omnipresence of laterally extensive erosional scours. It is nevertheless clear that these sequences consist of stacked-upwards-fining cycles, and lateral comparison of these show them to consists of (1) a basal nodular conglomerate overlying an erosional contact that, in turn, is (2) overlain by very fine-grained feldspathic wacke sheets and stacked, lenticular fine-grained feldspathic wacke, that (3) fines upward into a *Katbergia*-bioturbated nodule-bearing paleosol.

DISCUSSION

The present study confirmed several, but not all, of the basic lithostratigraphic characteristics of the Katberg Formation at Carlton Heights. Katberg sandstones are reported to be quartzitic and arenaceous (Johnson 1976, 1991; Hiller and Stavrakis 1984; Groenewald 1996; Retallack et al. 2003, their fig. 11); thus, the feldspathic nature of the sandstones in the area is unusual. The present study restricted sampling to the lowermost 100 + m of Katberg Formation at one locality and the mineralogy may reflect a local anomaly, although feldspathic wacke also has been reported from other P–Tr boundary sections elsewhere (i.e., Newbury et al. 2008; Gastaldo et al. 2009). Visser and Dukas (1979) and Johnson (1991) recognized an up-section increase in quartz content of the

TABLE 1.—*Sand:silt ratios, point-count, and mineralogical data determined using X-ray diffraction for lithofacies identified in the lowermost Katberg Formation, Carlton Heights.*

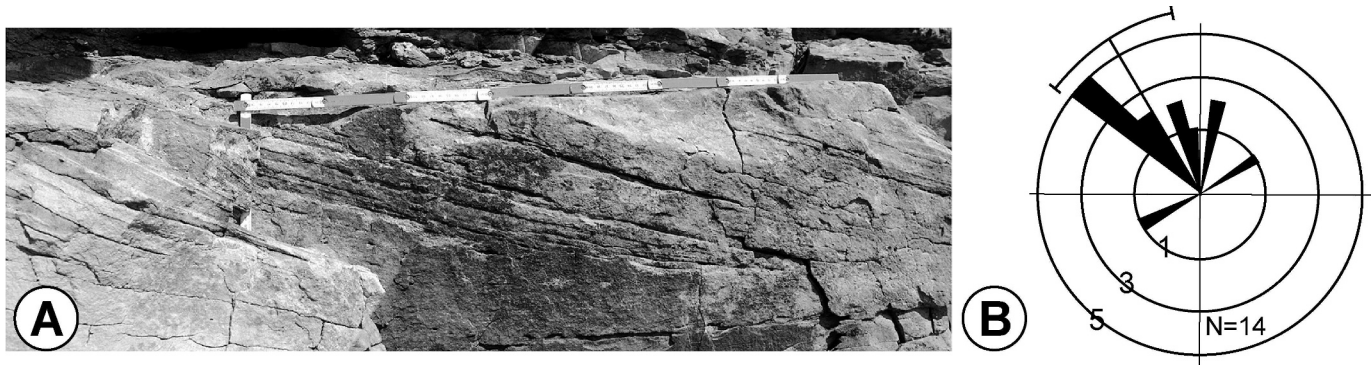|		Sand:Silt	Quartz	Feldspar	Lithic	Calcite	Clay (muscovite)	Mica
Pedogenic Conglomerate Nodules	XRD Bulk Mineralogy		10%	-	-	35%	55%	-
Fine Wacke	Point Count	55:45	33%	53%	14%	-	-	-
	XRD Bulk Mineralogy		10%	26.5%	-	-	-	62.9%
Very Fine Graywacke	Point Count	75:25	17%	76%	7%	-	-	-
	XRD Bulk Mineralogy		20.6%	66.5%	-	-	-	12.9%
Siltstone	XRD Bulk Mineralogy	-	2%	2%	-	-	96%	-

Fig. 8.—Sedimentary structures and paleocurrent. **A)** Trough cross-bedded sandstone characteristic of thick sandstone beds and used as the basis for paleocurrent analysis (viewed perpendicular to paleoflow). Scale in dm (white/gray) **B)** Rose-diagram plot of paleoflow measurements based on cross bedding and parting lineations using Oriana 2.0 software. General current direction is to the northwest; 10° sectors. $N = 14$.

Katberg Formation sandstones, a trend explained as the result of changing environmental conditions or provenance type.

The most important observations made in the present study at odds with previous reports are that: (1) two distinct sandstone facies exist in the

Fig. 9.— Sedimentary structures documented in very fine-grained sandstone sheets. **A)** Asymmetrical ripple marks. **B)** Polygonal, shallow desiccation cracks on the upper bounding surfaces of laminated sheet sandstone. **C)** Oblique view of desiccation cracks on top of decimeter-scale ripples on upper surface of barforms. Rippled surface is delimited by dotted line. Scale in dm and cm.

lowermost part of the formation; (2) individual sandstone bodies exhibit a multilateral channel-body architecture; (3) stacked multilateral sandstones amalgamate laterally due to landscape degradation, resulting in architectural elements that have been described as multistoried sandstone architectures (Smith 1995; Smith and Ward 2001; Ward et al. 2000; Ward et al. 2005); and (4) siltstones at Carlton Heights exhibit more mottling of green-gray and maroon colors than previously reported. The very fine-grained graywacke lithofacies has not been documented previously in the Katberg Formation. The erosional contacts in sandstone bodies, interpreted to have formed as the result of channel migration (Smith and Ward 2001; Maruoka et al. 2003; Steiner et al. 2003), are characteristic of only one of two lithofacies identified herein. Instead, many erosional surfaces in the stacked sandstones are linked to degradational phases of the landscape. Hence, the reported characterization that the Katberg Formation consists of multistoried sandstones is a function of sandstone-body amalgamation over very short lateral distances ($\sim$ 100 m), with these features exposed only in donga sections, which are the most resistant and easily accessible parts of the area. Although the nodular conglomerate lithofacies recognized in the present study has been used as a criterion to distinguish the Katberg Formation from underlying Permian sandstones, the nature of these nodules, when compared with other carbonate-cemented nodules in the formation, previously has gone unrecognized.

An important distinction must be made between the nodules (pisolith-size concretions; Fig. 5) found as channel lag deposits and those in *Katbergia*-bioturbated paleosols, based on their stable-isotope signatures (Fig. 10; Tabor et al. 2007; Gastaldo and Rolerson 2008). Stable isotope values of carbonate cements from pisolith-size channel-lag nodules (nodular conglomerate facies) record a geochemical system that was open with the atmosphere (δ^{13} C $> -10.6l$ ‰; Tabor et al. 2007). Hence, these nodules formed in paleosols that were in equilibrium with global tropospheric CO_2 (Tabor et al. 2007) and represent only residuum of aridisols (calcisols or gypsisols) wherein the nodules precipitated above the regional water table. In contrast, nodules found in *Katbergia*-bioturbated paleosols have δ^{13}C values that are < -10.6‰ (Tabor et al. 2007; Gastaldo and Rolerson 2008). These formed in wetland paleosols below the water table, isolated from the influence of atmospheric CO_2. This distinction, along with the macroscopic differences between nodule types, requires them to be interpreted independently when evaluating Early Triassic paleoenvironments and the climate under which they precipitated.

Carlton Heights is situated approximately 250–400 km from the Cape Fold Belt, which was the primary provenance of the Katberg Formation. Such a distant source for the carbonate nodules is unlikely because their chemical composition indicate a short transportation distance, an
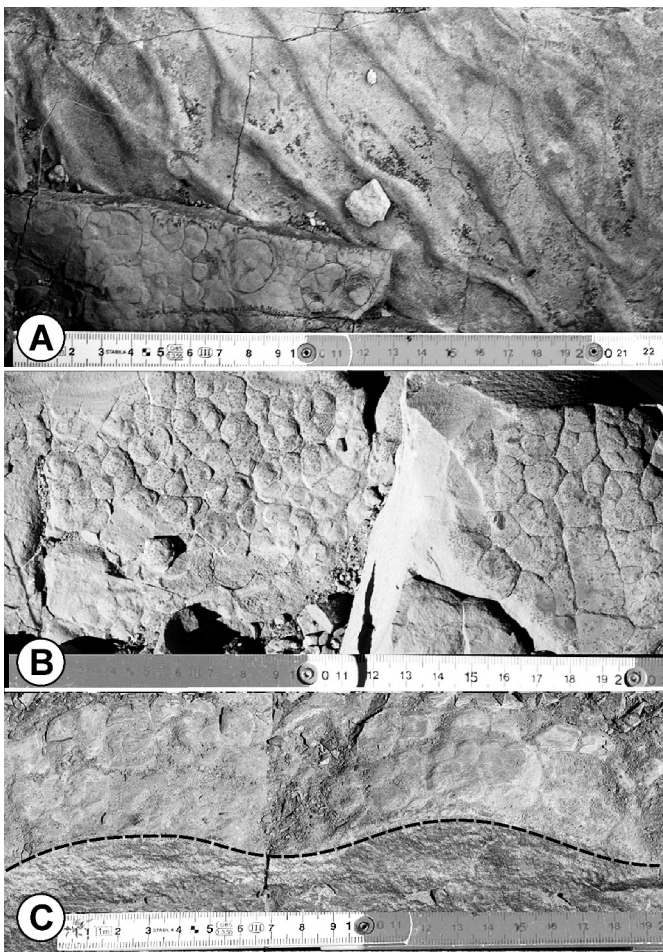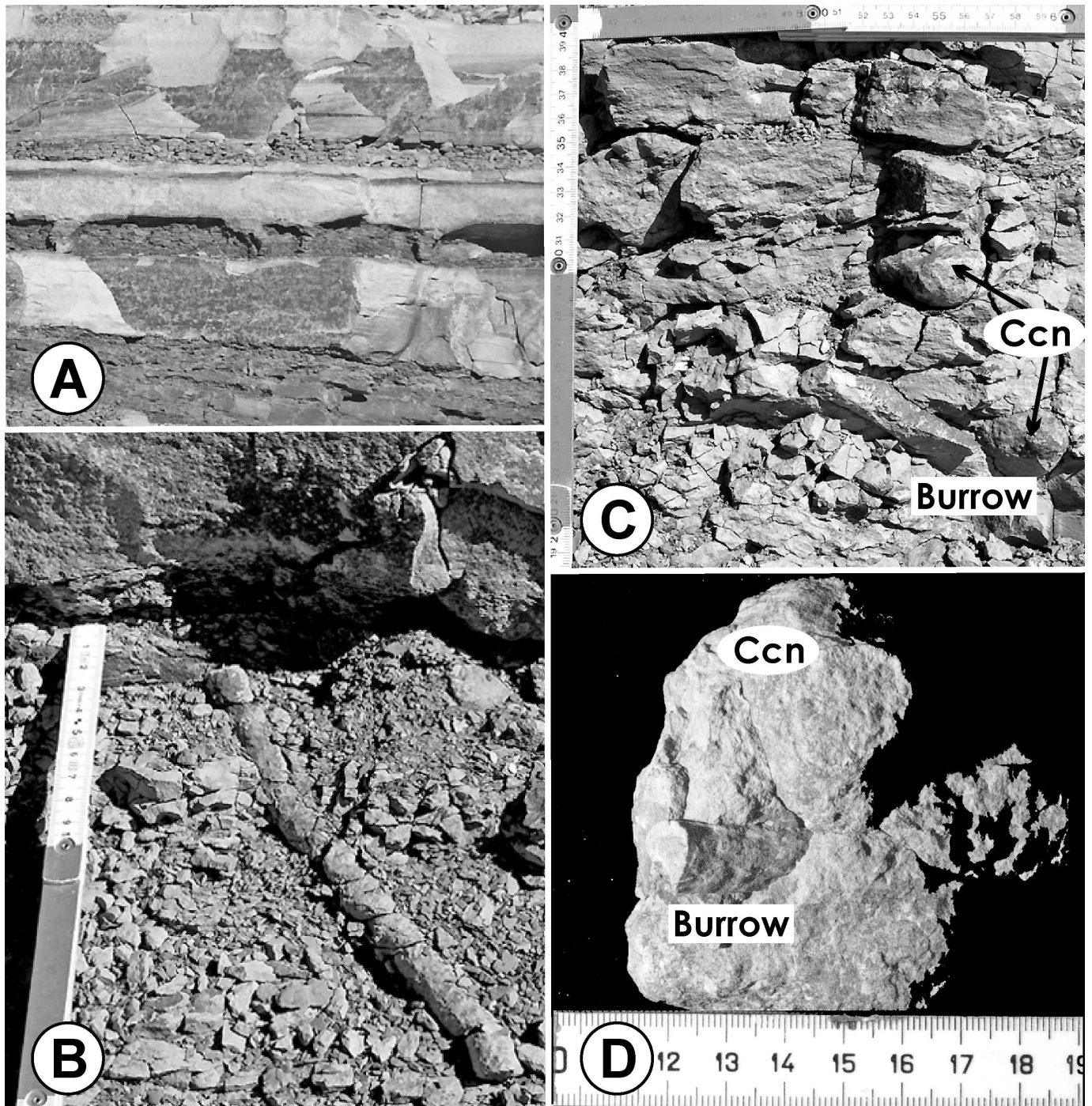
FIG. 10.—Sedimentary structures and ichnofossils. **A)** Sandstone-filled mudcracks that occur in a medium-thick lens of siltstone occurring in SS2. Similar sandstone-filled mudcracks are also found in siltstone facies beneath Ss3 (see Fig. 11B). **B)** Bioturbated siltstone with ornamented, siltstone-filled burrows assigned to *Katbergia* (Gastaldo and Rolerson 2008); scale in cm and dm. **C)** Siltstone-filled burrows associated with calcite concretions (Ccn) that are restricted to nodule horizons; scale in dm and cm. **D)** Calcite-cemented, siltstone-filled *Katbergia* burrow around which an authigenic calcite nodule formed. Scale in cm.

interpretation supported by the poor sorting (Fig. 5), the lateral and vertical extent of nodular conglomerate throughout the study area (Figs. 3, 11), and the thickness of individual cross-bedded nodular conglomerate bedsets (Fig. 6). Early Triassic calcisols (or aridisols) developed locally following aggradation of siltstone inceptisols that were overprinted as gleysols (Gastaldo and Rolerson 2008) during phases of increased seasonality, reduced rainfall, and overall climatic drying. Degradation of this more mature landscape resulted in erosion and

concentration of the residual calcareous nodules in basal channel lags, with the silt soils dispersed elsewhere in the basin.

A Model for Early Triassic Karoo Landscapes

Much of the recent research and hypotheses on the end-Permian extinction and documentation of post-extinction environments (Smith 1995; Ward et al. 2000; Ward et al. 2005; Smith and Ward 2001, p. 1147;
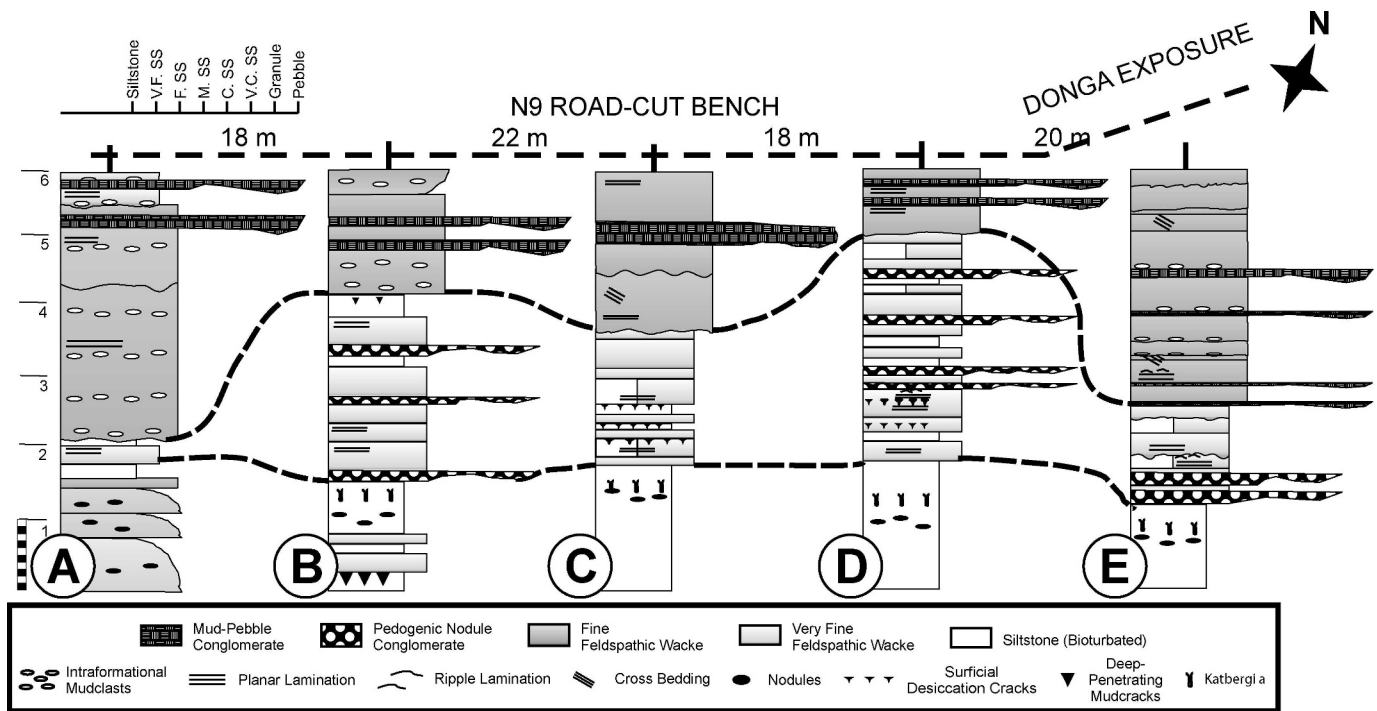
FIG. 11.—Stratigraphic sections drawn at five key localities in the third genetic unit as depicted in Figures 3 and 4 (uppermost sandstone bench; SS3, Fig. 4). Stratigraphic columns A–D are ordered from southwest to northeast; column E is the section from the donga exposure that is correlative to the roadcut bench (Fig. 2, CV). Scale = 1 m.

Smith and Botha 2005; Botha and Smith 2006) are based on the assumption that the stratigraphic record in the Karoo Basin is one of continuous sedimentation with no evidence of significant diastems or disconformities other than those normally found in fluvial sequences. In fact, Retallack et al. (2003) state that significant erosion in the carbonate-nodule-bearing intervals is unlikely because of high sediment-accumulation rates calculated for the stratigraphic interval. In contrast, the results of the present study demonstrate that sedimentation in the Karoo Basin was characterized by distinct periods of aggradation, equilibrium, and degradation during the Early Triassic (Figs. 12, 13; Gastaldo and Demko in press). The presence of two types of pedogenic nodules and relationship between calcisol (or aridisol) conglomerates, sheet sandstones, and bioturbated overbank interfluvial paleosols indicate alternating phases of high discharge and wetter conditions, and more seasonal and drier states.

A model is proposed to characterize each landscape and the corresponding climatic signature preserved therein (Fig. 14). Thick lenticular sandstones and floodplain fines deposited in vertically stacked beds, with little evidence of erosion, are characteristic of a rapidly aggrading system in a subhumid, probably wet seasonal, climate. Densely burrowed horizons in paleosols mark a shift from rapid aggradation to equilibrium (stasis) and a landscape dominated by extensive subaerially exposed floodplains (Fig. 14A, B). Gastaldo and Rolerson (2008) provide evidence to support moderate seasonality under which *Katbergia* colonized these substrates. Periodic increases in climatic moistening coincided with successive periods of rapid aggradation (Fig. 14C) and a rise in regional water table in response to potential accommodation. Subaerially exposed interfluves became inundated, animals responsible for *Katbergia* burrows abandoned their habitat, burrows were filled with multiple sedimentation events, and calcareous nodules formed at discrete horizons below the water table as inceptisols were overprinted as gleysols (Gastaldo and Rolerson 2008). Aggradation continued until landscape equilibrium was achieved; thereafter, pedogenesis was dominated by a

drier seasonal climate. At that point, calcisols developed on the interfluves when there was a drastic decrease in humidity and a correlative drop in the regional water table (Fig. 14E). The absence of *in situ* calcisols in the Early Triassic stratigraphy indicates that aggradational processes, alone, did not control floodplain deposition subsequent to the P–Tr event. Rather, these calcisols were scavenged during subsequent periods of regional degradation (Fig. 14F) when disequilibrium returned to the fluvial profile (e.g., Bull 1991; Quirk 1993). The largest clasts, carbonate nodules and intraformational mud clasts, were deposited in channel lags while the finer floodplain sediments were re-entrained and redeposited elsewhere in the system. This model conforms to the deposition of a complete genetic unit described in this study, but is frequently truncated by extensive local degradation which removed large portions of the Lower Triassic sequence.

Comparison with Fine-Grained Braided Systems

The findings of the present study are consistent with others interpretations of the Katberg Formation as a braided fluvial system (Hiller and Stavakis 1984; Smith and Ward 2001; Ward et al. 2000; Hancox et al. 2002) but differ from the classical braidplain due to a restricted range of grain size in the sediment load. The Katberg Formation, like the Westwater Canyon Member of the Morrison Formation, is much finer than that of other braided systems (Cowan 1991). It probably can be classified as a dryland anabranching system based on minimal vertical aggradation and a wide range of lateral and vertical accretionary features, although its architecture straddles the criteria presented by North et al. (2007) for discrete categorization.

One area today where clay-rich mud is transported in a network of low-gradient channels is Cooper Creek, central Australia (Nanson et al. 1986; Gibling et al. 1998). Here, two contemporaneous channel geometries exist under arid conditions. Braided low-sinuosity channels are dominated by bedload that consists of sand-size mud aggregates, which originated from
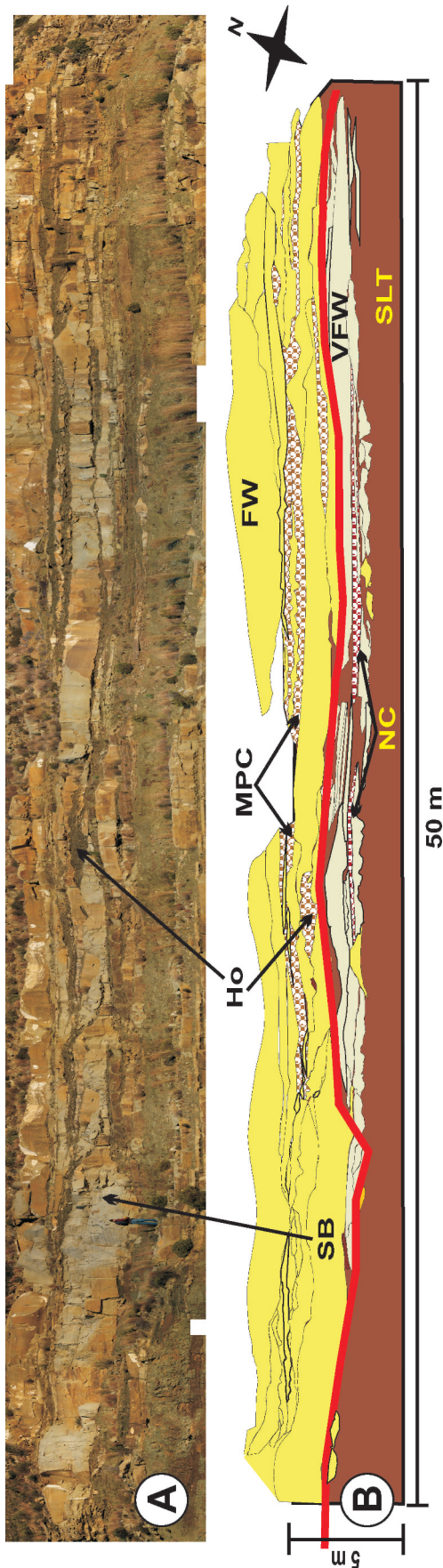
FIG. 12.—Illustrations of third sandstone bench (SS3) examined in Roadcut (RC; see Figs. 2, 4). **A)** Photomosaic including stratigraphic sections in Figure 11A–C wherein meso-scale features and sandstone geometries are shown. **B)** Line illustration of photomosaic in which bioturbated siltstone (SLT) is overlain by interbedded very fine-grained feldspathic lithic wacke (VFW) and nodular pebble conglomerate (NC). Troughs of individual fine-grained feldspathic wacke (FW) barforms (SB) are filled with mud-pebble conglomerate (MPC). Hollows (Ho) also are mud-pebble conglomerate filled. The fourth order bounding surface is marked in red, showing the extent of landscape degradation.

pedogenic activity on interfluves (Rust and Nanson 1989), and was transported as a function of their density (Margoulis and Nanson 1996) under lower flow systems. Anastamosing channels of various geometries (anabranching of North et al. 2007) are sand-clast dominated, and characterized by dune-and-ripple bedforms, with sediment load derived from erosion of subjacent Pleistocene deposits (Gibling et al. 1998). During the dry season, desiccation of calcic Vertisols (Gibling et al. 1998) results in mudcracks to depths of 1 m, which become apparent in the profile only when filled with sand. The lower parts of soil profiles, up to 2 m in depth, are reported to contain either small carbonate nodules (Rust and Nanson 1989) or carbonate or Fe/Mn oxide/hydroxide impregnations (Gibling et al. 1998). The mud-dominated system existing in the Channel Country of central Australia is believed to have begun ~ 100 ka with the onset of the last glacial episode.

When the Katberg Formation at Carlton Heights is compared with dryland settings in central Australia, only several aspects of the stratigraphy are compatible with the model. Early Triassic sandstone bodies are similar in that the predominant channel bedforms are dunes and ripples, with cross stratification commonly preserved (Figs. 8, 9, 12; Gibling et al. 1998). But, the multilateral nature of bedforms (Fig. 12) and intercalated pebble- to gravel-size mud clasts in interpreted hollows (Fig. 11) are not features identified in the Recent. Rather, mudclast sand-size aggregates of pedogenic origin coexist in contemporaneous low-sinuosity channels in the modern system (Nanson et al. 1986). Lithofacies lateral to the Katberg Formation feldspathic wacke channels consist of siltstone of various character in which there is evidence for wet interfluves on the basis of bioturbation (Gastaldo and Rolerson 2008), mottling, and stable-isotope geochemistry of carbonate nodules (Tabor et al. 2007). In contrast, calcic Vertisols have developed between contemporaneous channels in central Australia where carbonate and/or Fe/Mn soil nodules occur at depths from 20–50 cm (Gibling et al. 1998) up to 2 m (Rust and Nanson 1989). There are no data on the stable-isotope geochemistry from these nodules, although it is suspected that carbonate cements would be in isotopic equilibrium with the atmosphere, similar to that interpreted for the pisolith-size nodules found as channel-lag deposits at Carlton Heights (Tabor et al. 2007) and elsewhere in the Karoo Basin. Sand-filled mudcracks are prevalent in both feldspathic wacke (Fig. 10A) and siltstone (Fig. 11) facies, indicating seasonal drying, but depths are restricted to ~ 20 cm (compacted). Oscillation between wetter and drier climates in the Karoo Basin cannot be a function of glacial–interglacial forcing, inasmuch as continental glaciation ended in the Middle Permian (Montañez et al. 2007; Fielding et al. 2008).

One characteristic of the Early Triassic system that is not found in the Recent is the presence of pisolith-size pedogenic nodule-lag deposits confined to erosional channel bases and in overbank fines. Such features have been documented in other deep-time examples, mainly in calcic Vertisols of the Old Red Sandstone of Wales (Marriott and Wright 2006). Here, complete soil profiles consist of a surface (A) horizon characterized by crusts and desiccation cracks, a middle (B) horizon in which slickensides developed, and a lower (B_k or C_k) horizon in which small calcareous nodules precipitated in various morphologies. A complete soil is envisioned to range in thickness from 1 to 3 m, and aggradational processes resulted in the development of polyphase soil intervals (Marriott and Wright 2006). Rapid erosion of one or more soil profiles in the Old Red Sandstone resulted in the development of intraformational calcrete-clast conglomerates that appear to have remained within the interfluves (Marriott and Wright 2006, their fig. 3). Intraformational conglomerates are a common component and a key feature of the Katberg Formation, but they have not been found to be concentrated within overbank fines above the paleosol type in which they precipitated. Rather, intraformational nodular conglomerates record the only evidence for extreme aridity in this part of the basin (Tabor et al. 2007) as a residuum of those soils became concentrated either in channel lags
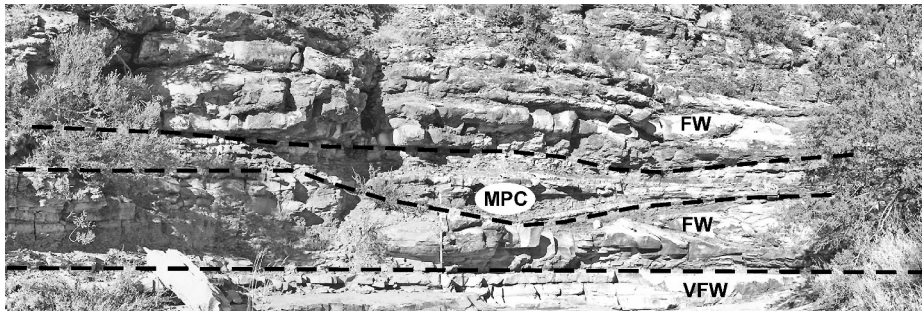
Fig. 13.—Photomosaic showing multiple, stacked aggradational and degradational sequences in the Katberg Formation. Contacts of degradational sequences are marked by dotted black lines. Photograph taken in VW donga (SS4; Fig. 3) above stratigraphic section illustrated in Figure 11E. Decimeter scale in center of photograph. VFW = very fine-grained feldspathic lithic wacke; FW = fine-grained feldspathic wacke; MPC = mud-pebble conglomerate.

(Figs. 3, 5), overbank fines (Fig. 11), or as barforms (Fig. 6). No paleosols have been found in which these precipitates occur *in situ*.

Factors Influencing Early Triassic Sedimentation in the Karoo Basin

The changeover from Late Permian meandering systems characteristic of the Palingkloof Member (Balfour Formation) to the Early Triassic Katberg braidplains traditionally was attributed to the impact of source-area uplift (Cole 1992; Catuneanu et al. 1998) combined with increasing aridity (Hiller and Stavrakis 1984; Smith 1995). More recently, the Early Triassic record has been interpreted in an environmental context where two competing hypotheses are advanced. Retallack et al. (2003) attributed the changeover in fluvial style to an increased sediment load, resulting in a change in climate to increasingly wet and higher precipitation regimes. In contrast, Ward et al. (2000) and Smith and Ward (2001) believed that a die-off of terrestrial vegetation, as a direct consequence of the P–Tr extinction event, resulted in the loss of rooted plants and consequent aridification. Extirpation promoted bank failure, re-entrainment of interfluvial sediments, and reworking of these into braidplains. Additionally, Ward et al. (2000) envisioned an increase in sediment load from denuded hill slopes, all under increasingly dry conditions.

The recent documentation of plant megafossils in the very fine-grained feldspathic wacke at Carlton Heights indicates that portions of the landscape were vegetated, casting doubt on a denuded Early Triassic (Gastaldo et al. 2005). This hypothesis also does not account for the fact that the Katberg Formation begins well above the top of the Permian in all sections examined. Hence, there does not appear to be any cause-and-effect relationship between the P–Tr extinction (as recognized by
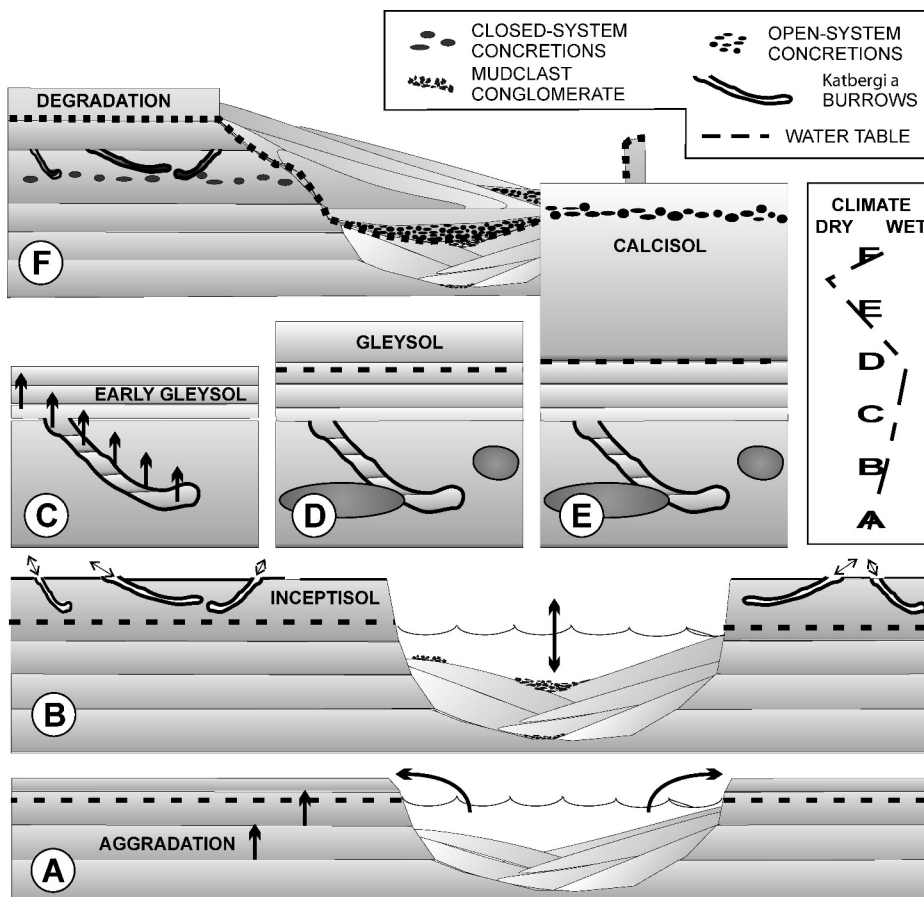

Fig. 14.—Model of aggradational and degradational cycles in the lower Katberg Formation as they relate to climate. A) Period of aggradation and high sedimentation rates under a wet climate. B) Phase of stasis during which little aggradation or degradation occurs, allowing colonization of the interfluves by burrowing arthropods (Gastaldo and Rolerson 2008). An inceptisol develops with the floodplain water table that remained below the base of the burrows. Pebble and cobble clasts consisting of siltstone eroded from the margin of the floodplain may accumulate within channels. C) Initiation of continued aggradation when overbank deposition fills abandoned burrows. D) Continued aggradation and concomitant water table rise, calcite cementation of burrow fills and matrix, as well as authigenic cementation of isotopically closed-system nodules (Tabor et al. 2007) indicative of a water-logged gleysol (Gastaldo and Rolerson 2008), the wettest conditions recorded in the Early Triassic. E) A period of stasis following aggradation under a drier climate where calcisols develop in the floodplain. Pebble-size calcitic nodules (Fig. 5) develop in the calcisol, with regional water table maintained at a depth above burrowed siltstones. Stable-isotope signature of pebble-size nodules indicates that these formed in a system open with atmospheric CO_2 (Tabor et al. 2007). F) Degradation of the calcisol landscape during the onset of a wetter climate phase and incision into older landscape(s). Pebble-size nodules are scavenged from floodplains and deposited as channel lags, whereas silt matrix is re-entrained either as pebble-to-cobble mud clasts or as suspension load sediment. Previous fluvial deposits are eroded and redeposited along with floodplain sediment within barforms of braided channel systems that may be superimposed over previous fluvial systems, resulting in stacked sandstones.

vertebrate biostratigraphy) and a shift in fluvial style in the Karoo Basin. The findings of the present study indicate that oscillations in climate, from wet conditions (under which inceptisols and gleysols developed across the interfluves—Sellwood and Price 1994; Cecil and DuLong 2003) to arid (under which calcisols formed—Sellwood and Price 1994; Cecil and DuLong 2003), occurred repeatedly throughout the lowest 100 + m of Katberg Formation stratigraphy. And, the first occurrence of nodular conglomerate, used to delimit the base of the Katberg Formation (Johnson 1976; Smith and Ward 2001; Smith and Botha 2005; Botha and Smith 2006) occurs ~ 15 m above the biostratigraphically defined P–Tr boundary at Carlton Heights (Gastaldo et al. 2005), indicating that there is missing section of at least one calcisol-dominated landscape that formed stratigraphically above the contact. Hence, there is no evidence for a single climatic shift that would have resulted in a one-time vegetational die-off that induced the onset of Katberg sedimentation.

The repetitive shifts between wetter and drier depositional environments (Fig. 14) indicate a climate that fluctuated from semihumid to semiarid for a prolonged period during which the lower Katberg Formation aggraded and degraded. Estimates by Retallack et al. (2003, p. 1145) propose that the average annual precipitation in the Early Triassic was 732 mm ± 141 mm, although these are based on depth to calcareous nodules using the assumption that only discrete paleosol types occur in the Karoo (see Gastaldo and Rolerson 2008). These data are difficult to reconcile with climate influences on sedimentation rate, for example, as recognized by Cecil et al. (2003). They note that sediment yield acts as a function of seasonality (number of wet months) instead of mean annual rainfall. And, with this in mind, Gastaldo and Demko (in press) reiterate the fact that the fluvial record is generated (or lost) only when the fluvial profile is in disequilibrium (e.g., Bull 1991; Quirk 1993; Posamentier and Allen 1999). Disequilibrium occurs during shifts in climate states under which pronounced seasonality occurs.

Intervals in the lower part of the Katberg Formation dominated by sheet sandstones, desiccation cracks, and the remnants of aridisols across the landscape are indicative of a prevailing semiarid (Sellwood and Price 1994), possibly monsoonal climate which would intimate a precipitation regime of 1–2.5 months/year. Highly mottled siltstone, in which carbonate nodules formed below the water table (Tabor et al. 2007), indicates a more seasonal and wetter climate than bioturbated paleosols (Sellwood and Price 1994). Inceptisols can form under any precipitation regime (Cecil and DuLong 2003), whereas gleysols (Gastaldo and Rolerson 2008) are most common when the precipitation regime is greater than 5 months/year. Peak sediment flux is achieved during shifts in climate towards increased precipitation (Demko et al. 2004), which is evidenced by an abundance of erosional surfaces and intraformational mud clasts (Rust and Legun 1983). The basal 100 + m of the Katberg Formation are dominated by these features. Hence, while the onset of a braidplain-dominated landscape in the Early Triassic of the Karoo Basin may have been induced by tectonic processes, it is concluded that the unique sedimentation style of the Katberg Formation was a function of strong climatic oscillations (cf. Milankovitch-scale) rather than pulses of orogenic activity or any ecosystem response to the P–Tr extinction. Finally, the stratigraphic section following the P–Tr boundary event in the main Karoo Basin at Carlton Heights represents an incomplete record, with an unknown thickness of sedimentary sequence removed before and during the development of the Katberg Formation braidplains.

CONCLUSIONS

The lower part of the Katberg Formation at Carlton Heights has been shown to be characterized by fine-grained, feldspathic, siliciclastic sedimentary systems that were deposited under climatic conditions that oscillated throughout the early Triassic. Two distinctive sandstone facies constitute the architectural elements identified in the area, with (1) fine-grained wackes and interbedded pebble–mudstone conglomerate interpreted as deposits in multilateral channels as barforms, and (2) very fine-grained graywacke in sheet-sandstone geometries interpreted as both within-channel and overbank (?levee) deposits. These are bounded by erosional channel bases containing pisolith-size nodular conglomerate, marking phases of landscape degradation under more seasonal climatic conditions. Mottled and bioturbated siltstone intervals, interpreted as overbank fines on interfluves, exhibit polyphase pedogenesis. *Katbergia*-burrowed intervals represent colonization under seasonally wet conditions in inceptisols, whereas the siltstone overprinted by large nodular concretions occurred under wetland conditions and high regional water tables. Continued landscape aggradation ultimately was capped by the development of aridisols in which pisolith-size carbonate nodules precipitated in equilibrium with atmospheric pCO_2 at some unknown depth below the air–soil interface. But, there is no evidence in the stratigraphy for aridisols (or calcicsols) except for the presence of these nodules concentrated into channel lags, barforms, and overbank lenses as the result of landscape degradation and scavenging under the return of seasonally wet conditions. Deposition of the lowermost Katberg Formation is considered to have been a function of oscillating climate rather than periodic orogenic pulses in the Cape Fold Belt. When compared with Recent dryland systems, characteristics of the Katberg Formation place it between categories identified by North et al. (2007) for anabranching systems. And, when compared with the Old Red Sandstone of Wales, an ancient dryland system, the Katberg Formation differs in that, to date, there is no evidence on the concentration of pedogenic carbonate nodules in the interfluves. Rather, it appears that the entire thickness of aridisols in the region were eroded and removed from the stratigraphic record. Inasmuch as evidence for the first aridisol following the P–Tr extinction event occurs only as a channel lag deposit ~ 15 m above that boundary as defined by vertebrate biostratigraphy, indicating the removal of an aridisol (or calcisol) landscape, there appears to be little evidence to support an origin of the Katberg Formation to have been a consequence of the die off of terrestrial plants as a consequence of the extinction.

REFERENCES

ABDALA, F., CISNEROS, J.C., AND SMITH, R.M.H., 2006, Faunal aggregation in the Early Triassic Karoo Basin: Earliest evidence of shelter-sharing behavior among tetrapods?: PALAIOS, v. 21, p. 507–512.

ALLEN, J.R.L., 1974, Studies in fluviatile sedimentation: implications of pedogenic carbonate units, Lower Old Red Sandstone, Anglo-Welsh outcrop. Geological Journal, v. 9, p. 181–208.

ALLEN, J.R.L., 1986, Pedogenic carbonates in the Old Red Sandstone facies (late Silurian–early Carboniferous) of the Anglo-Welsh area, southern Britain, *in* Wright, V.P., ed., Paleosols: Their Recognition and Interpretation: Oxford, U.K., Blackwell Scientific, p. 58–86.

BENTON, M.J., TVERDOKHLEVOBA, V.P., AND SURKOVA, M.V., 2004, Ecosystem remodelling among vertebrates at the Permian–Triassic boundary in Russia: Nature, v. 432, p. 97–100.

BOTHA, J., AND SMITH, R.M.H., 2006, Rapid vertebrate recuperation in the Karoo Basin of South Africa following the End-Permian extinction: Journal of African Earth Science, v. 45, p. 502–514.

BULL, W.B., 1991. Geomorphic Responses to Climatic Change: Oxford, U.K., Oxford University Press, 326 p.

CATUNEANU, O., AND BOWKER, D., 2001, Sequence stratigraphy of the Koonap and Middleton fluvial formations in the Karoo foredeep South Africa: Journal of African Earth Science, v. 33, p. 579–595.

CATUNEANU, O., AND ELANGO, H.N., 2001, Tectonic control on fluvial styles: the Balfour Formation of the Karoo Basin, South Africa: Sedimentary Geology, v. 140, p. 291–313.

CATUNEANU, O., HANCOX, P.J., AND RUBIDGE, B.S., 1998, Reciprocal flexural behaviour and contrasting strategies: A new basin development model for the Karoo retroarc foreland system, South Africa: Basin Research, v. 10, p. 412–438.

CECIL, C.B., AND DULONG, F.T., 2003, Precipitation models for sediment supply in warm climates, *in* Cecil, C.B., and Edgar, N.T., eds., Climate Controls on Stratigraphy: SEPM, Special Publication 77, p. 21–27.

CECIL, C.B., DULONG, F.T., HARRIS, R.A., COBB, J.C., GLUCKOTER, H.G., AND NUGROHO, H., 2003, Observations on climate and sediment discharge in selected tropical rivers, Indonesia, in Cecil, C.B., and Edgar, N.T., eds., Climate Controls on Stratigraphy: SEPM, Special Publications 77, p. 29–50.

COLE, D.I., 1992, Evolution and development of the Karoo Basin, *in* De Wit, M.J., and Ransome, I.G.D., eds., Inversion Tectonics of the Cape Fold Belt, Karoo and Cretaceous Basins of Southern Africa: Rotterdam, Balkema, p. 87–99.

COWAN, J.E., 1991, The large-scale architecture of the fluvial Westwater Canyon Member, Morrison Formation (Upper Jurassic), San Juan Basin, New Mexico, *in* Miall, A.D., and Tyler, N., eds., The Three-dimensional Facies Architecture of Terrigenous Clastic Sediments and Its Implications for Hydrocarbon Discovery and Recovery: SEPM, Concepts in Sedimentology and Paleontology, v. 3, p. 80–93.

DEMKO, T.M., CURRIE, B.S., AND NICOLL, K.A., 2004, Regional paleoclimatic and stratigraphic implications of paleosols and fluvial/overbank architecture in the Morrison Formation (Upper Jurassic), Western Interior, USA: Sedimentary Geology, v. 167, p. 115–135.

DE KOCK, M.O., AND KIRSCHVINK, J.L., 2004, Paleomagnetic constraints on the Permian–Triassic boundary in terrestrial strata of the Karoo Supergroup, South Africa: implications for causes of the End-Permian Extinction Event: Gondwana Research, v. 7, p. 175–183.

DE WIT, M.J., GOSH, J.G., DE VILLIERS, S., RAKATOSOLOFO, N., ALEXANDER, J., TRIPATHI, A., AND LOOY, C., 2002, Multiple organic carbon isotope reversals across the Permo-Triassic boundary of terrestrial Gondwana sequences: Clues to extinction patterns and delayed ecosystem recovery: Journal of Geology, v. 110, p. 227–240.

DU TOIT, A.L., 1917, The geology of part of the Transkei. Explanation of Cape Sheet 27 (Maclear–Umtata): Geological Survey of South Africa, 32 p.

ERWIN, D.H., 2006. Extinction: How Life on Earth Nearly Ended 250 Million Years Ago: Princeton, New Jersey, Princeton University Press, 296 p.

FIELDING, C.R., FRANK, T.D., BIRGENHEIER, L.P., RYGEL, M.C., JONES, A.T., AND ROBERTS, J., 2008, Stratigraphic imprint of the Late Palaeozoic Ice Age in eastern Australia: a record of alternating glacial and nonglacial climate regime: Geological Society of London, Journal, v. 65, p. 129–140.

GALFETTI, T., BUCHER, H., OVTCHAROVA, M., SCHALTEGGER, U., BRAYARD, A., BRÜHWILER, T., GOUDEMAND, N., WEISSERT, H., HOCHULI, P.A., CORDEY, F., AND GUODUN, K., 2007, Timing of the Early Triassic carbon cycle perturbations inferred from new U–Pb ages and ammonoid biochronozones: Earth and Planetary Science Letters, v. 258, p. 593–604.

GASTALDO, R.A., AND DEMKO, T.M., 2009, The relationship between continental landscape evolution and the plant-fossil record: long term hydrologic controls on preservation, *in* Bottjer, D.J., and Allison, P.A., eds., Temporal Trends in Taphonomic Processes: Berlin, Germany, Springer Verlag, Topics in Geobiology, v. 37, p. 199–2020.

GASTALDO, R.A., AND ROLERSON, M.W., 2008, *Katbergia* gen. nov., a new trace fossil from the Late Permian and Early Triassic of the Karoo Basin: implications for paleoenvironmental conditions at the P/Tr extinction event: Palaeontology, v. 51, p. 215–229.

GASTALDO, R.A., ADENDORFF, R., BAMFORD, M., LABANDEIRA, C.C., NEVELING, J., AND SIMS, H., 2005, Taphonomic trends of macrofloral assemblages across the Permian–Triassic Boundary, Karoo Basin, South Africa: Palaios, v. 20, p. 479–497.

GASTALDO, R.A., NEVELING, J., CLARK, C.K., AND NEWBURY, S.S., 2009, The terrestrial Permian–Triassic boundary event bed is a non-event: Geology, v. 37, p. 199–202.

GIBLING, M.R., 2006, Width and thickness of fluvial channel bodies and valley fills in the geological record: A literature compilation and classification: Journal of Sedimentary Research, v. 76, p. 731–770.

GIBLING, M.R., NANSON, G.C., AND MAROULIS, J.C., 1998, Anastomosing river sedimentation in the Channel Country of central Australia: Sedimentology, v. 45, p. 595–619.

GRADSTEIN, F.M., OGG, J.O., AND SMITH, A.G., eds., 2004, A Geologic Time Scale: Cambridge, U.K., Cambridge University Press, 500 p.

GROENEWALD, G.H., 1996, Stratigraphy of the Tarkastad Subgroup, Karoo Supergroup, South Africa [Unpublished Ph.D. Thesis]: University of Port Elizabeth: South Africa, 145 p.

HANCOX, P.J., BRANDT, D., REIMOLD, W.U., KOEBERL, C., AND NEVELING, J., 2002, Permian–Triassic boundary in the Northwest Karoo basin: Current stratigraphic placement, implications for basin development models, and the search for evidence of impact, *in* Koeberl, C., and MacLeod, K.G., eds., Catastrophic Events and Mass Extinctions: Impacts and Beyond: Geological Society of America, Special Paper 356, p. 429–444.

HASIOTIS, S.T., 2000, The invertebrate invasion and evolution of Mesozoic soil ecosystems: the ichnofossil record of ecological innovations, *in* Gastaldo, R.A., and DiMichele, W.A., eds., Phanerozoic Terrestrial Ecosystems: The Paloentological Society, Papers, v. 6, p. 141–169.

HILLER, N., AND STAVRAKIS, N., 1980, Distal alluvial fan deposits in the Beaufort Group of the Eastern Cape: Geological Society of South Africa, Transactions, v. 83, p. 353–360.

HILLER, N., AND STAVRAKIS, N., 1984, Permo-Triassic fluvial systems in the Southeastern Karoo basin, South Africa: Palaeogeography, Palaeoclimatology, Palaeoecology, v. 45, p. 1–21.

JOHNSON, M.R., 1966, The stratigraphy of the Cape and Karoo Systems in the Eastern Cape Province [unpublished M.Sc. Thesis]: Rhodes University: Grahamstown, South Africa, 76 p.

JOHNSON, M.R., 1976, Stratigraphy of the Cape and Karoo Systems in the Eastern Cape Province [unpublished Ph.D. Thesis]: Rhodes University: Grahamstown, South Africa, 336 p.

JOHNSON, M.R., 1991, Sandstone petrography, provenance and plate tectonic setting in Gondwana context of the southeastern Cape-Karoo Basin: South African Journal of Geology, v. 94, p.137–154.

JOHNSON, M.R., VAN VUUREN, C.J., VISSER, J.N.J., COLE, D.I., WICKENS, H.DEV., CHRISTIE, A.D.M., AND ROBERTS, D.L., 1997, The Foreland Karoo Basin, South Africa, *in* Selley, R.C., ed., Sedimentary Basins of the World: New York, Elsevier, p. 169–185.

MACLEOD, K.G., SMITH, R.M.H., KOCH, P.L., AND WARD, P.D., 2000, Timing of mammal-like reptile extinctions across the Permian–Triassic boundary in South Africa: Geology, v. 28, p. 227–230.

MARAIS, J.A.H., AND JOHNSON, M.R., 1965, Thickness of the Cape and Karoo Systems in the Eastern Cape: Annals of the Geological Survey, South Africa, v. 4, p. 49–55.

MARGOULIS, J.C., AND NANSON, G.C., 1996, Bedload transport of aggregated muddy alluvium from Cooper Creek, central Australia: a flume study: Sedimentology, v. 43, p. 771–790.

MARRIOTT, S.B., AND WRIGHT, V.P., 2006, Investigating paleosol completeness and preservation in mid-Paleozoic alluvial paleosols: A case study in paleosol taphonomy from the Lower Old Red Sandstone, *in* Alonso-Zarza, A.M., and Tanner, L.H., eds., Paleoenvironmental Record and Application of Calcretes and Palustrine Carbonates: Geological Society of America, Special Paper 416, p. 43–52.

MARUOKA, T., KOERBERL, C., HANCOX, P.J., AND REIMOLD, U.W., 2003, Sulfur geochemistry across a terrestrial Permian–Triassic boundary section in the Karoo Basin, South Africa: Earth and Planetary Science Letters, v. 206, p. 101–117.

MIALL, A.D., 1996. the Geology of Fluvial Deposits; Sedimentary Facies, Basin Analysis, and Petroleum Geology: New York, Springer-Verlag, 582 p.

MONTAÑEZ, I.P., TABOR, N.J., NIEMEIER, D., DIMICHELE, W.A., FRANK, T.D., FIELDING, C.R., AND ISBELL, J.L., 2007, CO$_2$-Forced climate and vegetation instability during Late Paleozoic deglaciation: Science, v. 315, p. 87–91.

MUNDIL, R., LUDWIG, K.R., METCALFE, I., AND RENNE, P.R., 2004, Age and timing of the Permian Mass Extinctions: U/Pb dating of closed-system zircons: Science, v. 305, p. 1760–1763.

NANSON, G.C., RUST, B.R., AND TAYLOR, G., 1986, Coexistent mud braids and anastomosing channels in an arid-zone river: Cooper Creek, central Australia: Geology, v. 14, p. 175–178.

NEVELING, J., 2004, Stratigraphic and sedimentological investigation of the contact between the *Lystrosaurus* and the *Cynognathus* Assemblage Zones (Beaufort Group: Karoo Supergroup): Council for Geoscience, Pretoria, Bulletin 137, 165 p.

NEWBURY, S.S., CLARK, C.K., GASTALDO, R.A., AND NEVELING, J., 2008, High Resolution stratigraphy of the Permian–Triassic boundary at Bethulie, Karoo Basin, South Africa (abstract): Geological Society of America, Abstracts with Program, v. 396, 148 p.

NORTH, C.P., NANSON, G.C., AND FAGAN, S.D., 2007, Recognition of the sedimentary architecture of dryland anabranching (anastomosing) rivers: Journal of Sedimentary Research, v. 77, p. 925–938.

OVTCHAROVA, M., BUCHER, H., SCHALTEGGER, U., GALFETTI, A., BRAYARD, J., AND GUEX, J., 2006, New early to middle Triassic U-Pb ages from South China: Calibration with ammonoid biochronozones and implications for the timing of the Triassic biotic recovery: Earth and Planetary Science Letters, v. 243, p. 463–475.

POSAMENTIER, H.W., AND ALLEN, G.P., 1999, Siliciclastic Sequence Stratigraphy; Concepts and Applications: SEPM, Concepts in Sedimentology and Paleontology, no. 6, 210 p.

QUIRK, D.G., 1993, Base profile: A unifying concept in alluvial sequence stratigraphy, *in* Howell, J.A., and Aitken, J.F., eds., High Resolution Sequence Stratigraphy: Innovations and Applications: Geological Society of America, Special Publication 104, p. 37–49.

RETALLACK, G.J., SMITH, R.M.H., AND WARD, P.D., 2003, Vertebrate extinction across Permian–Triassic boundary in Karoo Basin, South Africa: Geological Society of America, Bulletin, v. 115, p. 1133–1152.

RUST, B.R., 1978, A classification of alluvial channel systems, *in* Miall, A.D., ed., Fluvial Sedimentology: Canadian Society of Petroleum Geologists, Memoir 5, p. 187–198.

RUST, B.R., AND LEGUN, A.S., 1983, Modern anastomosing-fluvial deposits in arid central Australia and a Carboniferous analogue in New Brunswick, Canada, *in* Collinson, J.D., and Lewin, J., eds., Modern and Ancient Fluvial Systems: International Association of Sedimentologists, Special Publication 6, p. 385–392.

RUST, B.R., AND NANSON, G.C., 1989, Bedload transport of mud as pedogenic aggregates in modern and ancient rivers: Sedimentology, v. 36, p. 291–306.

SELLWOOD, B.W., AND PRICE, G.D., 1994, Sedimentary facies as indicators of Mesozoic palaeoclimate, *in* Allen, J.R.L., Hoskins, B.J., Sellwood, B.W., Spicer, R.A., and Valdes, P.J., eds., Palaeoclimates and Their Modelling, with Special Reference to the Mesozoic Era: London, Chapman and Hall, p. 79–88.

SCHEFFLER, K., HOERNES, S., AND SCHWARK, L., 2003, Global changes during Carboniferous–Permian glaciation of Gondwana: Linking polar and equatorial climate evolution by geochemical proxies: Geology, v. 31, p. 605–608.

SOUTH AFRICAN COMMITTEE FOR STRATIGRAPHY (SACS), 1980, Stratigraphy of South Africa, Part 1. Lithostratigraphy of the Republic of South Africa, South West Africa/ Namibia, and the Republics of Bophuthawana, Trarnskei, and Venda. Handbook 8: Pretoria, South Africa, Geological Survey of South Africa, 690 p.

SMITH, R.M.H., 1987, Morphology and depositional history of exhumed Permian point bars in the southwestern Karoo, South Africa: Journal of Sedimentary Petrology, v. 57, p. 19–29.

SMITH, R.M.H., 1993, Vertebrate taphonomy of Late Permian floodplain deposits in the Southwestern Karoo Basin of South Africa: PALAIOS, v. 8, p. 45–67.

SMITH, R.M.H., 1995, Changing fluvial environments across the Permian–Triassic boundary in the Karoo basin, S. Africa and possible causes of tetrapod extinctions: Palaeogeography, Palaeoclimatology, Palaeoecology, v. 117, p. 81–104.

SMITH, R.M.H., AND BOTHA, J., 2005, The recovery of terrestrial vertebrate diversity in the South African Karoo Basin after the end-Permian extinction: Compte Rendu Palevol, v. 4, p. 555–568.

SMITH, R.M.H., AND WARD, P.D., 2001, Pattern of vertebrate extinctions across an event bed at the Permian–Triassic boundary in the Karoo Basin of South Africa: Geology, v. 28, p. 227–230.

SMITH, R.M.H., ERICKSON, P.A., AND BOTHA, W.J., 1993, A review of the stratigraphy and sedimentary environments of the Karoo-aged basins of Southern Africa: Journal of African Earth Science, v. 16, p. 143–169.

STEAR, W.M., 1985, Comparison of the bedform distribution and dynamics of modern and ancient sandy ephemeral flood deposits in the southwestern Karoo region, South Africa: Sedimentary Geology, v. 45, p. 209–230.

STEINER, J.B., ESHET, Y., RAMPINO, M.R., AND SCHMINDT, D.M., 2003, Fungal abundance spike and the Permian–Triassic boundary in the Karoo Supergroup (South Africa): Palaeogeography, Palaeoclimatology, Palaeoecology, v. 194, p. 405–414.

TABOR, N.J., MONTAÑEZ, I.P., STEINER, M.B., AND SCHWINDT, D., 2007, $\delta^{13}C$ values of carbonate nodules across the Permian–Triassic boundary in the Karoo Supergroup (South Africa) reflect a stinking sulfurous swamp, not atmospheric CO_2: Palaeogeography, Palaeoclimatology, Palaeoecology, v. 252, p. 370–381.

VISSER, J.N.J., AND DUKAS, B.A., 1979, Upward fining fluviatile megacycles in the Beaufort Group north of Graaff Reinet, Cape Province: Transactions of the Geological Society of South Africa, v. 82, p. 149–154.

WARD, P.D., MONTGOMERY, D.R., AND SMITH, R.M.H., 2000, Altered river morphology in South Africa related to the Permian–Triassic extinction: Science, v. 289, p. 1740–1743.

WARD, P.D., BOTHA, J., BUICK, R., DE KOCK, M.O., ERWIN, D.H., GARRISON, G., KIRSCHVINK, J., AND SMITH, R.H.M., 2005, Abrupt and gradual extinction among Late Permian land vertebrates in the Karoo Basin, South Africa: Science, v. 307, p. 79–714.

WRIGHT, P.W., AND MARRIOTT, S.B., 2007, The dangers of taking mud for granted: Lessons from Lower Old Red Sandstone dryland river systems of South Wales: Sedimentary Geology, v. 195, p. 91–100.